

Discovery of 1,3,4-Oxadiazole Derivatives as Broad-Spectrum Antiparasitic Agents

Alexandra Ioana Corfu,[†] Nuno Santarem,^{§,♦} Sara Luelmo,^{§,♦} Gaia Mazza,[∇] Alessandro Greco,[⊥] Alessandra Altomare,[†] Giulio Ferrario,[†] Giulia Nasta,[†] Oliver Keminer,^{§,‡} Giancarlo Aldini,[†] Lucia Tamborini,[†] Nicoletta Basilico,[∇] Silvia Parapini,[¶] Sheraz Gul,^{§,‡} Anabela Cordeiro-da-Silva,^{§,♦} Paola Conti,[†] Chiara Borsari^{†,*}

[†]Department of Pharmaceutical Sciences, University of Milan, Via Mangiagalli 25, 20133 Milan, Italy

[§]Institute for Research and Innovation in Health (i3S), University of Porto, 4200-135 Porto, Portugal

[♦]Department of Biological Sciences, Faculty of Pharmacy, University of Porto, Rua de Jorge ViterboFerreira 228, 4050-313 Porto, Portugal

[∇]Department of Biomedical, Surgical and Dental Sciences, Via Pascal 36, 20133 Milan, Italy

[⊥]Department of Pharmacy, University of Pisa, Via Bonanno 6, 56126 Pisa, Italy

[§]Fraunhofer Institute for Translational Medicine and Pharmacology ITMP, Schnackenburgallee 114, 22525 Hamburg, Germany

[‡]Fraunhofer Cluster of Excellence for Immune-Mediated Diseases CIMD, Schnackenburgallee 114, 22525 Hamburg, Germany

[¶]Department of Biomedical Sciences for Health, Via Pascal 36, 20133 Milan, Italy

*Correspondence to: chiara.borsari@unimi.it, Dept. of Pharmaceutical Sciences, University of Milan; Via Mangiagalli 25, 20133 Milan, Italy. Tel. +39 02503 19309.

ABSTRACT

Vector-borne parasitic diseases (VBPDs) pose a significant threat to public health on a global scale. Collectively, Human African Trypanosomiasis (HAT), Leishmaniasis and Malaria threaten millions of people particularly in developing countries. Climate change might alter the transmission and spread of VBPDs, leading to a global burden of these diseases. Thus, novel agents are urgently needed to expand the therapeutic options and limit the spread of drug-resistance parasites. Herein, we report the development of broad-spectrum antiparasitic agents, by screening a known library of antileishmanial and antimalarial compound towards *Trypanosoma brucei* (*T. brucei*) and identifying a 1,3,4-oxadiazole derivative (**19**) as anti-*T. brucei* hit with predicted blood-brain-barrier permeability. Subsequently, extensive Structure-Activity-Relationship studies around the lipophilic tail of **19**, led to a potent antitrypanosomal and antimalarial compound (**27**), with moderate potency also towards *Leishmania infantum* (*L. infantum*) and *L. tropica*. In addition, we discovered a pan-active antiparasitic molecule (**24**), showing low micromolar IC₅₀s towards *T. brucei* and *Leishmania* spp. promastigotes and amastigotes, and nanomolar IC₅₀ against *Plasmodium falciparum*, together with high selectivity for the parasites over mammalian cells (THP-1). Early ADME-toxicity assays were used to assess the safety profile of the compounds. Overall, we characterized **24** and **27**, bearing the 1,3,4-oxadiazole privileged scaffold, as broad-spectrum low-toxicity agents for the treatment of VBPDs. An alkyne-substituted chemical probe (**30**) was synthesized and will be utilized in proteomics experiments aimed at deconvoluting the mechanism of action in *T. brucei* parasite.

KEYWORDS

Vector-borne parasitic diseases; Human African Trypanosomiasis; Leishmaniasis; Malaria; Broad-spectrum molecules; ADME-Tox; 1,3,4-oxadiazole.

Vector-borne parasitic diseases (VBPDs) are a group of infections which include Human African Trypanosomiasis (HAT), Leishmaniasis and Malaria. These diseases represent a significant global health problem and threaten millions of people particularly in developing countries. Despite being highly prevalent in tropical and subtropical regions, climate changes are expected to adversely impact the transmission dynamics of vector-borne diseases and shift the disease burden across the world.¹ HAT is caused by infection with two subspecies of the protozoan parasite *Trypanosoma brucei* (*T. brucei gambiense* or *T. brucei rhodesiense*) and is fatal if not treated.^{2,3} The vector of *T. brucei* subspecies is the tsetse fly of the genus *Glossina*.⁴ Leishmaniasis is transmitted by sandflies and caused by a variety of *Leishmania* species. Leishmaniasis usually presents in three different forms: visceral (VL), cutaneous or mucocutaneous with 700 000 to 1 million new cases occurring annually.⁵ Malaria is a mosquito-borne disease caused by five protozoa of the genus *Plasmodium* and transmitted by the bite of infected anopheline mosquitoes. Infections with *Plasmodium falciparum* (*P. falciparum*) are responsible for >90% of malaria mortality worldwide, and according to the World Health Organisation (WHO), malaria cases reached 249 million in 2022.⁶ Despite the serious health, economic, and social consequences of infections, the available treatments are associated with drawbacks including toxicity, poor efficacy, and serious side effects.^{7,8} Due to the lack of funding for VBPD drug research and development, public-private partnerships have filled this gap shifting the landscape of VBPD research, and helping to decrease the disease threat on a global scale.⁹⁻¹² However, the widespread resistance of these protozoan parasites to current drugs, results in an urgent need to identify new classes of antiparasitic agents. The drug discovery process targeting *T. brucei*, *Leishmania* spp. and *P. falciparum* faces challenges due to the complex biology of these organisms, which can involve intracellular stages or affect the central nervous system (CNS).

Phenotypic approaches in VBPD drug discovery are powerful as they allow identification of compounds that are active against the entire parasite, as they simultaneously take into account the ability of compound to modulate a disease causing target at the molecular level, but also membrane permeability, cell uptake and efflux mechanisms.¹³⁻¹⁷ To this end, phenotypic screening has been successfully applied in the field of VBPDs, as demonstrated by the discovery of fexinidazole and acoziborole for the treatment of HAT, GSK3186899 and DNDI-0690 for Leishmaniasis, and cipargamin

for the treatment of malaria. Fexinidazole (Figure 1A) is an orally available 2-substituted 5-nitroimidazole compound that was identified through a phenotypic screening of a DNDi chemical library by Swiss TPH, and further developed by Hoechst (now Sanofi). Following the positive scientific opinion granted by the European Medicines Agency in 2018, the WHO included fexinidazole in the guideline for the treatment of both first- and second-stage HAT caused by *T. brucei gambiense*.^{18, 19} In addition, fexinidazole was granted FDA approval in 2021. Acoziborole (Figure 1A), formerly known as SCYX-7158, represents another successful example of the exploitation of cell-based phenotypic screenings for the identification of novel drug candidates. It is an orally-active benzoxaborole that has been advanced to phase II/III clinical trials for the treatment of HAT.^{20, 21}

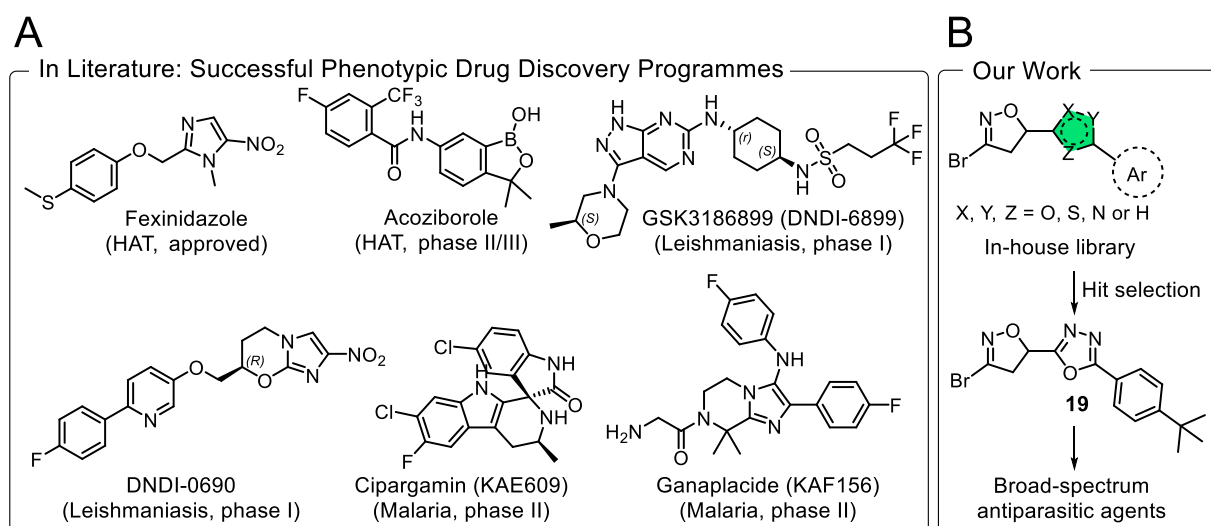


Figure 1. A) Chemical structure and development phase of a selection of antitrypanosomal, antileishmanial and antimalarial agents. **B)** Workplan aimed at identifying broad-spectrum antiparasitic agents.

Whole-cell phenotypic assays have been used also to identify molecules active against *Leishmania* species. GlaxoSmithKline (GSK) performed a high-throughput screening on >1 million compounds towards *Leishmania donovani* (*L. donovani*), the major causative agent of VL, and identified 192 compounds with antileishmanial activity (“Leish-Box”).²² A collaborative effort between the GSK Global Health Unit and the University of Dundee Drug Discovery Unit undertaking optimization of a VL phenotypic hit led to GSK3186899 as a high quality clinical candidate (DNDI-6899, DDD853651; <https://clinicaltrials.gov> NCT03874234, see chemical structure in Figure 1A).²³ In addition, phenotypic screenings of repurposed drug libraries have yielded many potentially novel antileishmanial compounds. An antitubercular nitroimidazo-oxazole derivative (DNDI-VL-2098) has been repurposed for neglected

tropical diseases (NTDs) after its unexpected inhibitory activity towards *L. donovani*, with efficacy in both mouse and hamster models of VL after oral administration.²⁴ Despite the promising results in preclinical studies, the development of DNDI-VL-2098 was halted due to the discovery of a link between dose, length of treatment, and testicular toxicity. Despite this drawback, the phenotypic screening of the nitroimidazole library of the TB Alliance allowed the DNDI to pinpoint another phenotypic hit for VL, DNDI-0690 (Figure 1A).²⁵ Due to its superior safety profile, DNDI-0690 was progressed to phase I clinical trials for VL (NCT03929016).

Phenotypic screening has the potential to deliver the next-generation antimalarial agents, as demonstrated by the discovery of cipargamin (KAE609, Figure 1A), which is currently undergoing phase II clinical trial for the treatment of *P. falciparum* malaria (NCT03334747).²⁶ KAE609 is a synthetic spiroindolone discovered by a public-private partnership (Novartis Institute for Tropical Diseases and Medicines for Malaria Venture) through the optimization of a phenotypic hit.^{27, 28} Another example of a drug candidate originating from phenotypic screen is ganaplacide (KAF156, Figure 1A).²⁹ This compound is an imidazolopiperazine-based compound with low nanomolar IC₅₀s against the *Plasmodium* parasites, and currently undergoing phase IIb clinical trials (NCT03167242) in combination with lumefantrine, a known antimalarial drug.

Despite the recent advancements in the field, there is an urgent need for the discovery of additional therapeutic options for the treatment of HAT, leishmaniasis and malaria. Herein, we report the results of a medicinal chemistry campaign aimed at identifying novel broad-spectrum antiparasitic agents. The initial chemical starting point was identified following a phenotypic screening that made use of an in-house compound library of known antimalarial and antileishmanial agents³⁰ towards *T. brucei* parasite, and led to the identification of the 1,3,4-oxadiazole derivative (**19**) as anti-*T. brucei* hit compound (Figure 1B). When considering the impact of *T. brucei* on the CNS, a multiparameter optimization (CNS MPO) desirability tool was exploited to predict blood-brain-barrier (BBB) permeability, and the resulting CNS MPO score was used to prioritize hit selection. Subsequently, we performed a Structure-Activity Relationship (SAR) study around the lipophilic tail of **19**, and the novel library (compounds **20-29**) was investigated towards *T. brucei*, two *Leishmania* spp., namely *L. tropica* and *L. infantum*, and *P. falciparum*. Counter-screening of the compounds against mammalian cells (THP-1) allowed the

exclusion of cytotoxic compounds, and early ADME-Tox assays allowed the identification of compounds **24** and **27** as promising antiparasitic agents for the treatment of vector-borne parasitic infections.

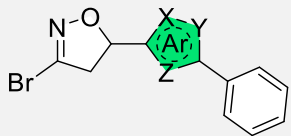
RESULTS AND DISCUSSION

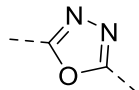
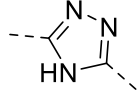
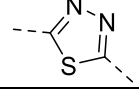
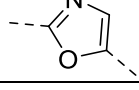
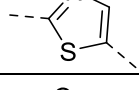
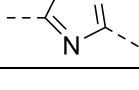
T. brucei Phenotypic Screening of the In-House Library

An in-house library of nineteen compounds (**1-19**), which previously showed antimalarial and antileishmanial activity,³⁰ was assessed for its potency against the bloodstream form of *T. brucei* parasite. In addition, these compounds were evaluated for cytotoxicity in THP-1 macrophage-like cells to evaluate cell toxicity and calculate the half maximal cytotoxicity concentration (CC_{50}) and the Selectivity Index ($SI = CC_{50}/IC_{50}$ parasite). At first, we investigated the effect of the heteroaromatic ring connecting the 3-bromo-4,5-dihydroisoxazole (BDHI) moiety with the phenyl ring. The 1,3,4-oxadiazole- and 1,2,4-triazole-substituted compounds (**1** and **2**) inhibited *T. brucei* cell growth with IC_{50} of 22.06 and 19.54 μ M, respectively. Increasing the partition coefficient ($clogP$) in compounds **3-6**, we observed a slight improvement in the potency against *T. brucei* ($IC_{50} = 10-12$ μ M). All tested compounds (**1-6**) did not show toxicity towards THP-1, with CC_{50} higher than 100 μ M, resulting in Selectivity Indexes higher than 9 and 10 (Table 1).

Despite removal of systemic infection might be beneficial for host survival, during stage 2 HAT infection the parasites reach the CNS leading to sleep disturbances, paralysis, progressive dementia and death. To predict the suitability of our molecules to cross the BBB, the CNS MPO score was calculated based on six physicochemical properties: (i) molecular weight (MW); (ii) lipophilicity, calculated partition coefficient ($clogP$); (iii) calculated distribution coefficient at pH 7.4 ($clogD$); (iv) topological polar surface area (TPSA); (v) number of hydrogen-bond donors (HBDs); and (vi) most basic center (pK_a).³¹ Compounds with CNS MPO > 5 are expected to pass the BBB and exhibit pharmacological activity in the CNS.³² With the exception of the thiazole derivative **5**, this set of compounds showed CNS MPO > 5 and a TPSA between 40 and 90 \AA^2 , which is desirable for BBB penetration.³¹

Table 1. SAR study on the heteroaromatic core.

Comp.	Ar	IC_{50} <i>T. brucei</i> (μ M) and (range)	CC_{50} (μ M)	SI	$clogP^a$	TPSA ^a (\AA^2)	CNS MPO ^a
							

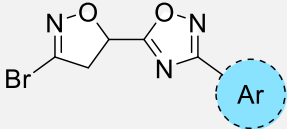
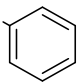
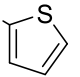
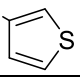
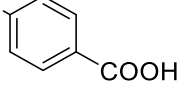
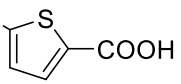
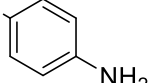
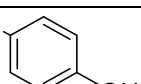
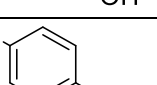
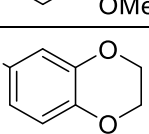
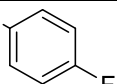
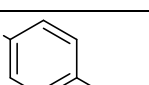
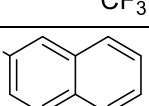
1		22.06 (18.72-25.87)	>100	>4	1.80	60.51	6
2		19.54 (16.14-23.53)	>100	>5	1.74	63.16	5.75
3		12.06 (8.93-15.51)	>100	>8	2.60	47.37	5.70
4		10.30 (8.63-12.44)	>100	>10	2.30	47.62	5.85
5		10.84 (8.89-12.85)	>100	>9	3.49	34.48	4.74
6		10.64 (8.43-13.00)	>100	>9	3.25	60.51	5.25

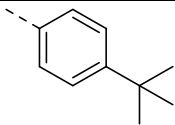
Data depicted are the calculated IC₅₀ and associated 95% confidence interval from the merged data sets from at least three independent experiments for *T. brucei*; the CC₅₀ and associated 95% confidence interval from the merged data sets from at least three independent experiments for THP-1 cells; the selectivity index (SI): IC₅₀ toward the parasite compared with compound cytotoxicity CC₅₀ on host cells (CC₅₀/C₅₀). ^aMarvin/JChem 20.9 was used to calculate logD (distribution coefficient) or logP (partition coefficient) values, topological polar surface area (TPSA, Å²), and CNS multiparameter optimization (CNS MPO) values; ChemAxon (<https://www.chemaxon.com>).

To gain insight into the role of the aromatic substituent on potency and selectivity, we selected the 1,2,4-oxadiazole as template and screened a library of compounds bearing different aromatic and heteroaromatic moieties towards *T. brucei* parasites (Table 2). The phenyl/thiophene bioisosteric replacement (compounds **6** and **7/8**) led to a decrease in the anti-*T. brucei* potency. The introduction of a carboxylic group on both the phenyl (**9**) and thiophene (**10**) ring resulted in a complete loss of potency (IC₅₀ > 40 μM), which might be related to the lack of cellular permeability due to the negatively charged carboxylate at physiological pH (cLogD_{7.4}: **9** = -0.51; **10** = -0.84, Table 2). The presence of an amino or hydroxyl group on the phenyl ring resulted in moderately active compounds (IC₅₀ **11** = 25.42 μM; **12** = 14.48 μM). Replacement of the hydroxyl group with a methoxy substituent (comp. **13**) led to a 3-fold improvement in anti-*T. brucei* potency, however **13** showed only a limited selectivity for *T. brucei* parasite over THP-1 (SI = 9). Introduction of lipophilic groups, such as a fluorine (**15**), trifluoromethyl

(**16**) and *tert*-butyl (**18**) moieties, produced potent and selective inhibitors, with compound **18** being the best one (IC_{50} **18** = 2.42 μ M; SI = 28, Table 2). However, the highly lipophilic compounds **16-18** displayed a CNS MPO < 5, which is not desirable for BBB penetration and for treating stage 2 HAT.

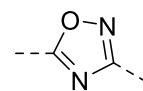
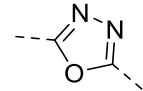
Table 2. SAR Study on aromatic substituent on the 1,2,4-oxadiazole core.

							
Comp.	Ar	IC_{50} <i>T. brucei</i> (μ M) and (range)	CC_{50} (μ M) and (range)	SI	clogD ^a	TPSA ^a (\AA^2)	CNS MPO ^a
6		10.64 (8.43-13.00)	>100	>9	3.25	60.51	5.25
7		21.85 (17.67-25.06)	>100	>4	2.89	60.51	5.56
8		17.30 (14.08-20.87)	>100	>5	2.99	60.51	5.51
9		>40	>100	>2	-0.51	97.81	5.49
10		>40	>100	>2	-0.84	97.81	5.49
11		25.42 (18.38-33.75)	>100	>4	2.47	86.53	5.27
12		14.48 (11.04-18.39)	>100	>7	2.97	80.74	5.27
13		5.36 (4.43-6.39)	49.73 (44.89-54.92)	9	3.05	69.74	5.45
14		13.52 (11.41-16.00)	68.84 (63.39-74.74)	5	2.68	78.97	5.66
15		4.55 (3.33-5.83)	>100	>22	3.39	60.51	5.11
16		3.29 (2.57-4.02)	>100	>30	4.13	60.51	4.42
17		4.29 (3.48-5.17)	67.67 (64.29-71.33)	16	4.25	60.51	4.38

18		2.42 (2.11 – 2.75)	41.22 (29.90-57.06)	28	4.84	60.51	4.08
See legend Table 1.							

With the aim of selecting a hit compound with high probability of BBB penetration, compound **18** was compared to its corresponding 1,3,4-oxadiazole derivative (**19**, Table 3). The 1,3,4-regioisomers are known to show an improved lipophilicity profile and more favorable ADME-Tox properties with respect to their corresponding 1,2,4-oxadiazoles.³³ Indeed, the 1,3,4-oxadiazole isomer **19** displayed an order of magnitude lower lipophilicity (cLogP: **18** = 4.84; **19** = 3.35, Table 2) compared to the 1,2,4-oxadiazole derivative **18**, resulting in an optimal CNS MPO score (5.15, Table 3). For these reasons, we selected the 1,3,4-oxadiazole scaffold and we performed a SAR study to investigate the effect of the lipophilic tail on compound activity and selectivity.

Table 3. Comparison between 1,2,4- and 1,3,4-oxadiazole bearing compounds.

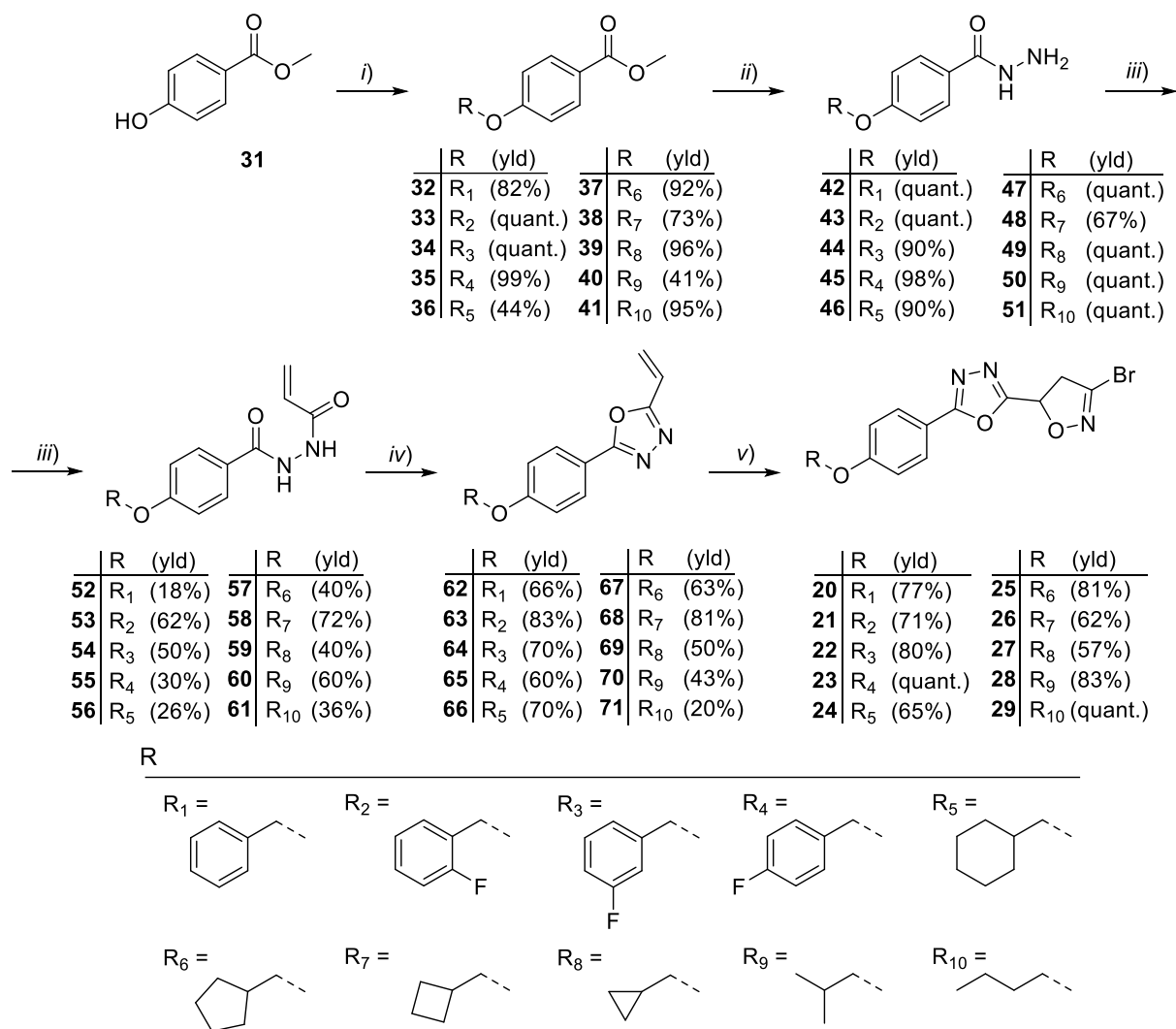
Comp.	Ar	IC ₅₀ <i>T. brucei</i> (μ M) and (range)	CC ₅₀ (μ M) and (range)	SI	clogD ^a	TPSA ^a (\AA^2)	CNS MPO ^a
18		2.42 (2.11-2.75)	41.22 (29.90-57.06)	28	4.84	60.51	4.08
19		5.61 (4.96-6.33)	60.68 (50.01-71.98)	11	3.35	60.51	5.15

See legend Table 1.

Chemistry

The library of novel 1,3,4-oxadiazole derivatives (**20-29**) was synthesized as depicted in Scheme 1. The Williamson ether synthesis was used to convert the commercially available methyl 4-hydroxybenzoate (**31**) into the corresponding ethers **32-41**, by treating it with the desired alkyl bromides,

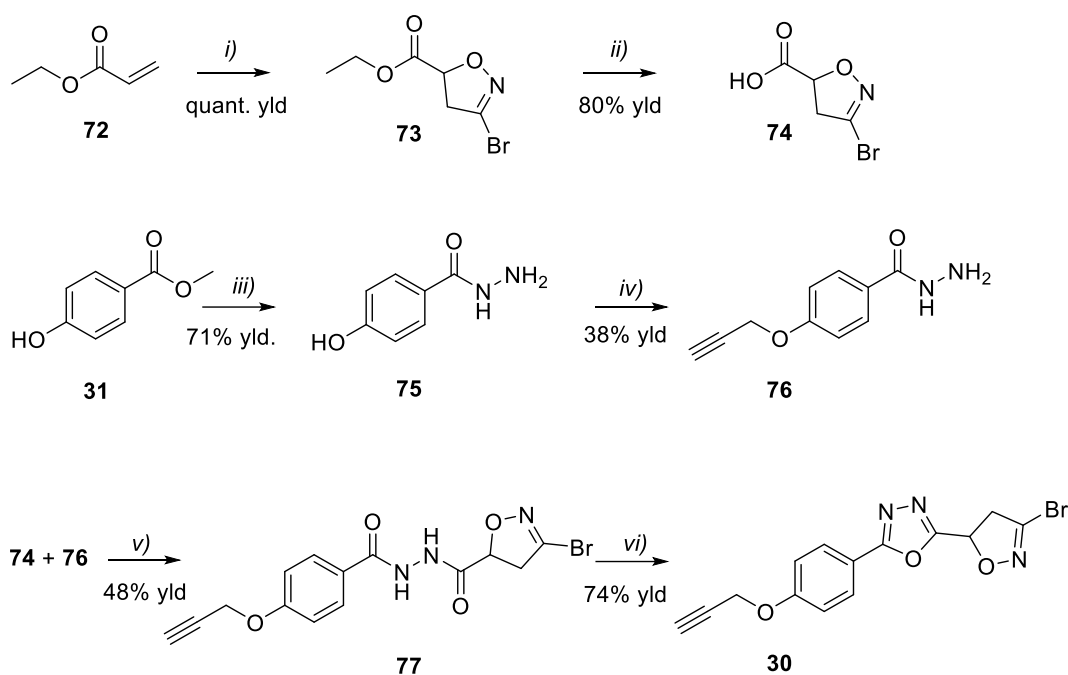
in the presence of solid K_2CO_3 as a base, in refluxing acetone. This reaction generally proceeded with good yield with a few exceptions (Scheme 1). In the case of the cyclopentanemethyl derivative **37**, the poor reaction yield required the use of a different synthetic procedure. A Mitsunobu reaction between methyl 4-hydroxybenzoate **31** and cyclopentanemethanol, in the presence DIAD and PPh_3 , afforded compound **37** in a 92% yield. Esters **32-41** were then converted into their respective hydrazides **42-51** by refluxing them in the presence of hydrazine hydrate in ethanol. The subsequent chemoselective *N*-acylation with acrylic acid, EDC·HCl in dry dichloromethane at room temperature afforded derivatives **52-61**. The *N*-acylated derivatives were submitted to a cyclization reaction³⁴ using hexachloroethane, *N,N*-diisopropylethylamine and triphenylphosphine in acetonitrile at room temperature to afford the 2,5-disubstituted 1,3,4-oxadiazoles **62-71**. These intermediates are characterized by the presence of a vinyl substituent in the 2 position, which represents a good dipolarophile for the subsequent 1,3-dipolar reaction that was used to build the 3-bromo-4,5-dihydroisoxazole (BDHI) nucleus.³⁰ Indeed, alkenes **62-71** reacted with bromonitrile oxide, generated *in situ* from its stable precursor dibromoformaldoxime (DBF) in the presence of solid $NaHCO_3$ as heterogenous base and ethyl acetate as organic solvent, to give the final compounds **20-29** in good to quantitative yield (57% - quantitative).



Scheme 1. Synthesis of compounds **20-29**. Reagents and conditions: (i) R-Br, K₂CO₃, acetone, reflux, o/n (for **32-36**, **38-41**); or PPh₃, DIAD, cyclopentanemethanol, dry THF, o/n (for **37**); (ii) N₂H₂·H₂O (65%), EtOH, reflux, o/n; (iii) acrylic acid, EDC·HCl, DCM, r.t., o/n; (iv) DIPEA, hexachloroethane, PPh₃, ACN, r.t., o/n; (v) NaHCO₃, DBF, EtOAc, r.t., o/n.

For the synthesis of the molecular probe **30** (Scheme 2), it was necessary to follow a different synthetic pathway, since the alkyne group present on the R substituent would react as a dipolarophile in the cycloaddition reaction, leading to the corresponding 3-Br-isoxazole. Thus, two synthons **74** and **76** were separately prepared and then coupled using standard conditions (EDC·HCl, HOBT, TEA) leading to intermediate **77**. Finally, **77** was cyclized by treatment with hexachloroethane, *N,N*-diisopropylethylamine and triphenylphosphine in acetonitrile to yield the desired probe (**30**) in a 74% yield (Scheme 2). Carboxylic acid **74** was obtained in two steps and 80% yield from the commercially

available ethyl acrylate, which was submitted to 1,3-dipolar cycloaddition with DBF, followed by ester hydrolysis with a 1M aqueous solution of NaOH and dioxane. For the synthesis of **76**, we initially followed the same approach used to obtain hydrazides **42-51** by performing the Williamson ether synthesis as the first step and then refluxing with hydrazine hydrate in ethanol. However, under these conditions, reduction of the alkyne to the corresponding alkane was observed, due to the reducing properties of hydrazine.³⁵ Therefore, the methyl 4-hydroxybenzoate **31** was first converted into the corresponding hydrazide **75**, after which, O-alkylation of the phenol group with propargyl bromide, K₂CO₃ in acetone afforded the desired synthon **76**.



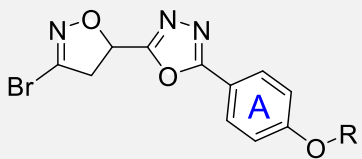
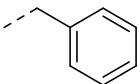
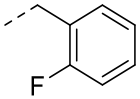
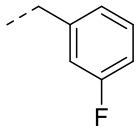
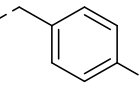
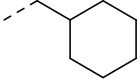
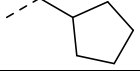
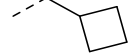
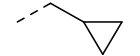
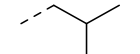
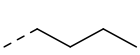
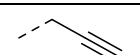
Scheme 2. Synthesis of compound **30**. Reagents and conditions: (i) DBF, NaHCO₃, EtOAc, r.t., o/n; (ii) 1M NaOH, dioxane; (iii) N₂H₂·H₂O (65%), MeOH, reflux, o/n; (iv) propargyl bromide, K₂CO₃, acetone, reflux, o/n; (v) EDC·HCl, HOBT, TEA, dry DCM, r.t., o/n; (vi) DIPEA, hexachloroethane, PPh₃, ACN, r.t., o/n.

SAR Study and Anti-*T. brucei* Agent Selection

The *tert*-butyl moiety of compound **19** was replaced with different lipophilic moieties, and an ether functionality was exploited to connect the phenyl ring (A in Table 4) with the desired substituent. The ether group was selected for the synthetic feasibility (see Scheme 1) and its ability to modulate

lipophilicity. All compounds present a 3-bromo-4,5-dihydroisoxazole (BDHI) moiety, which is a moderately reactive electrophile able to covalently engage cysteine residues.³⁶⁻³⁸ We also designed and synthesized a probe (**30**) that will be exploited for chemical proteomics experiments aimed at target identification. The probe **30** possesses an alkyne group that can be exploited to install, through a click-chemistry reaction, a visualization or enrichment tag, enabling subsequent analysis of the bound proteins. The library of ether-bridged compounds (**20-30**) bearing different aliphatic and aromatic moieties as lipophilic tails were tested against the bloodstream form of *T. brucei* parasite. The introduction of a benzyl group (**20**) and an *ortho*-fluorinated benzyl moiety (**21**) led to slightly less potent compounds compared to **19** (Table 4). Moving the fluorine from *ortho* (**21**) to *meta* (**22**) position resulted in a 2-fold increase in anti-*T. brucei* activity, and in a SI of 21. All benzyl-substituted compounds (**20-23**) displayed a clogP > 3.50 and CNS MPO < 5. Compound **24**, bearing a cyclohexane, was 3 times more potent than the corresponding aromatic derivative **20** (IC₅₀ **24** = 2.41 μM vs **20** = 7.24 μM). Considering the excellent activity of **24**, we decreased the size of the aliphatic ring aiming to reduce both lipophilicity and molecular mass aiming to facilitate the free diffusion through the BBB. The cyclopentyl-, cyclobutyl- and cyclopropyl-substituted compounds (**25-27**) showed no cytotoxicity in THP-1 macrophage-like cells (CC₅₀ > 100 μM), with the cyclopropyl derivative **27** showing the highest potency and selectivity (IC₅₀ = 2.73 μM; SI > 37, Table 4). Replacement of the cyclopropyl moiety with a branched (**28**) or linear (**29**) alkane chain led to a reduced activity towards the bloodstream form of *T. brucei* parasite, even though all compounds maintained IC₅₀ < 7 μM. The cycloalkyl- and alkyl-substituted compounds **26-29** displayed a CNS MPO > 5 and TPSA equal to 69.74 Å² (Table 4). Indeed, the most potent and selective molecule (**27**) fulfils the requirements for BBB penetration, including cLogP between 1.5 and 2.7 (2.42 for compound **27**), MW < 400 (364.2 for **27**) and TPSA between 40 and 90 Å² (69.74 Å² for **27**). In addition, compound **27** displays zero hydrogen bond donors (HBD), increasing the likelihood to identify a CNS-penetrant molecule as the number of HBD is suggested to be ≤ 1.³² The alkyne-substituted compound **30** maintained anti-*T. brucei* activity, highlighting that it can be exploited as chemical probe for target(s) identification.

Table 4. SAR study on the lipophilic tail of 1,3,4-oxadiazole bearing compounds.

							
Comp.	R	IC ₅₀ <i>T. brucei</i> (μ M) and (range)	CC ₅₀ (μ M) and (range)	SI	clogP ^a	TPSA ^a (\AA^2)	CNS MPO ^a
19	-	5.61 (4.96-6.33)	60.68 (50.01-71.98)	11	3.35	60.51	5.15
20		7.24 (5.91-8.70)	>100	>14	3.37	69.74	4.84
21		6.86 (6.03-7.77)	80.50 (67.65-113.9)	12	3.51	69.74	4.57
22		3.04 (2.69-3.41)	64.77 (53.46-80.16)	21	3.51	69.74	4.57
23		3.82 (3.29-4.43)	65.20 (52.13-87.97)	17	3.51	69.74	4.57
24		2.41 (2.16-2.69)	64.16 (54.50-76.87)	27	3.76	69.74	4.41
25		5.66 (4.93-6.46)	>100	>18	3.31	69.74	4.96
26		5.01 (4.24-5.89)	>100	>20	2.87	69.74	5.44
27		2.73 (2.46-2.98)	>100	>37	2.42	69.74	5.76
28		6.76 (5.19-8.56)	>100	>15	2.89	69.74	5.51
29		4.57 (3.98-5.28)	>100	>22	2.97	69.74	5.47
30		4.87 (4.35-5.46)	>100	>20	1.87	69.74	6

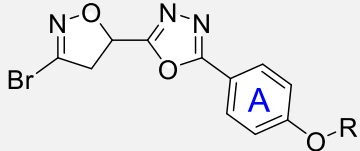
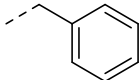
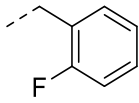
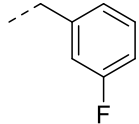
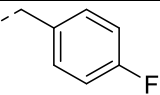
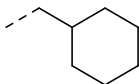
See legend Table 1.

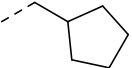
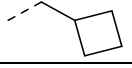
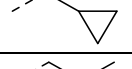
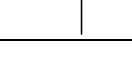
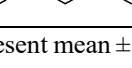
Investigation of Anti-Leishmanial Potency

Considering the potency towards *T. brucei*, we investigated the ability of our compounds to inhibit the growth of *Leishmania* parasites. A phenotypic assay on *L. tropica* and *L. infantum* promastigotes was performed using the MTT (3-(4,5-dimethylthiazol-2-yl)-2,5-diphenyltetrazolium bromide) method.³⁹ While *L. tropica* is the etiologic agents of cutaneous leishmaniasis, *L. infantum* causes VL.

With the exception of the *meta*-fluorinated benzyl derivative (**22**, IC₅₀ > 40 μM), the *ortho*- and *para*-F-substituted compounds (**21** and **23**) displayed a moderate antileishmanial activity towards *L. infantum* (**21** and **23**, IC₅₀ = 17-18 μM). As a general trend, the compounds were more potent towards *L. infantum* with respect to *L. tropica* parasites (Table 5). Replacing the aromatic ring of compound **20** with a cyclohexane (comp. **24**) led to a significant increase in antileishmanial activity (IC₅₀ *L. infantum*: **22** > 40 μM; **24** = 5.95 μM). Decreasing the size of the cyclic alkane diminished the ability of the compounds to inhibit the growth of *Leishmania* spp. parasites. Indeed, the cyclopropyl- (**27**), cyclobutyl- (**26**), cyclopentyl- (**25**) derivatives yielded a 2/3-fold decrease in anti-*L. infantum* potency compared to the cyclohexane-substituted compound **24**. Both compounds **24** and **27** displayed a broad-spectrum antiparasitic activity with IC₅₀ in the low micromolar range. The most potent and selective anti-*T. brucei* agent (comp. **27**, IC₅₀ = 2.73 μM; SI > 37, Table 4) resulted also in moderate antileishmanial activity (IC₅₀ *L. infantum* = 15.96 μM; SI > 6, Table 5), while **24** showed an analogue potency towards all three parasites (IC₅₀ *T. brucei* = 2.41 μM; *L. infantum* = 5.95 μM; and *L. tropica*: 8.98 μM), being promising agents for the broad-spectrum treatment of kinetoplastid infections.

Table 5. Antileishmanial activity of the novel library of compounds.

							
Comp.	R	<i>L. infantum</i> ^a IC ₅₀ ± SD (μM)	CC ₅₀ (μM) and range	SI	<i>L. tropica</i> ^a IC ₅₀ ± SD (μM)	SI	clogP ^b
20		>40	>100	-	>40	-	3.37
21		17.14 ± 6.41	80.50 (67.65-113.9)	5	24.73 ± 8.67	3	3.51
22		>40	64.77 (53.46-80.16)	-	>40	-	3.51
23		18.82 ± 10.47	65.20 (52.13-87.97)	4	29.93 ± 9.09	2	3.51
24		5.95 ± 1.56	64.16 (54.50-76.87)	11	8.98 ± 2.75	7	3.76

25		13.44 ± 5.16	>100	-	20.24	-	3.31
26		10.63 ± 3.53	>100	>9	20.86 ± 8.30	>5	2.87
27		15.96 ± 4.38	>100	>6	26.19 ± 12.01	>4	2.42
28		>40	>100	-	>40	-	2.89
29		13.99 ± 5.53	>100	>7	20.76 ± 4.33	>5	2.97

^aData represent mean ± standard deviation of three independent experiments. *Leishmania* spp. (*L. infantum* and *L. tropica*) promastigotes were used. The CC₅₀ and associated 95% confidence interval from the merged data sets from at least three independent experiments for THP-1 cells. Selectivity index (SI): IC₅₀ toward the parasite compared with compound cytotoxicity IC₅₀ on host cells (CC₅₀/IC₅₀). ^bMarvin/JChem 20.9 was used to calculate logD (distribution coefficient) or logP (partition coefficient) values, ChemAxon (<https://www.chemaxon.com>).

While the first screening was performed on the free living and easily cultured promastigote stage (insect-infective), the best performing compound (**24**) was tested against the clinically relevant and difficult to culture intra-macrophage amastigote stage (mammal-infective). The cyclohexyl-substituted derivative **24** was able to decrease the viability of *L. infantum* intracellular forms. **24** was tested against intracellular amastigotes at different concentrations and the IC₅₀ value was calculated. Compound **24** showed potent inhibition of *Leishmania* amastigotes (IC₅₀ = 8.18 μM), with an IC₅₀ comparable to that observed against promastigotes (IC₅₀ = 5.95 μM). Representative images of infected macrophages treated with **24** at 10 μM are reported in Figure 2. Moreover, **24** turned out to be more potent than the parental compound **19** (IC₅₀ = 17.19 μM).

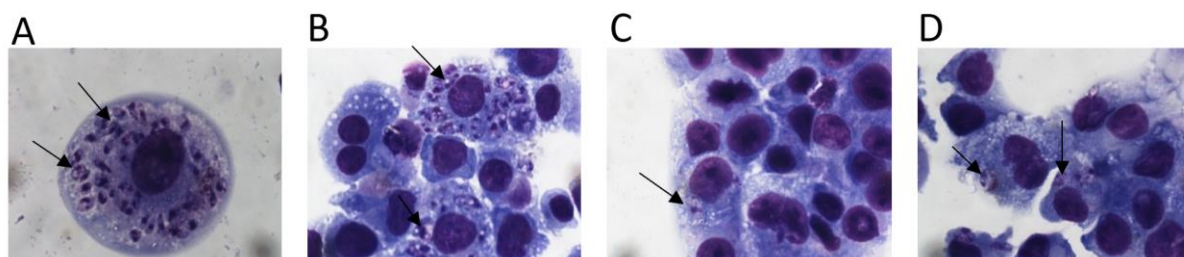


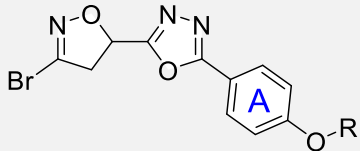
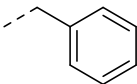
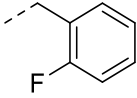
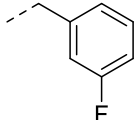
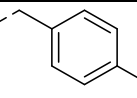
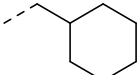
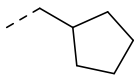
Figure 2. A-D) Antileishmanial activity of compound **24** against intracellular *Leishmania* amastigotes. Infected macrophages were exposed to compound **24** for 72 h. **A, B)** Microscopic imaging (x1000) of Giemsa stained *L. infantum* infected non-treated cells (control) macrophages showing numerous intracellular amastigotes.

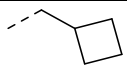
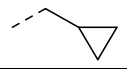
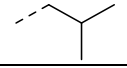
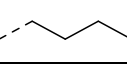
C, D) *L. infantum* infected macrophages treated with **24** at 10 μM showing reduction of amastigote burden. Amastigotes are indicated by arrows.

Evaluation of Anti-Malarial Potency

The novel library of 1,3,4-oxadiazole derivatives was tested against *P. falciparum* to determine their *in vitro* potency. The antimalarial activity was determined against chloroquine (CQ) sensitive (D10) and CQ resistant (W2) strains by measuring parasite viability after 72 hr of incubation with the compounds. All molecules showed comparable activity towards D10 and W2 strains, with IC_{50} in the nanomolar range and excellent selectivity indexes ($\text{SI} > 170$, Table 6). Interestingly, the most potent antileishmanial agent (compound **24**) turned out to be also the most potent compound towards *P. falciparum* W2 strain (IC_{50} **24** = 0.155 μM).

Table 6. Activity against D10 (CQ-S) and W2 (CQ-R) strains of *P. falciparum*.

							
Comp.	R	D10 ^a $\text{IC}_{50} \pm \text{SD}$ (μM)	CC_{50} (μM) and range	SI	W2 ^a $\text{IC}_{50} \pm \text{SD}$ (μM)	SI	clogP^{b}
20		0.307 ± 0.051	>100	>326	0.397 ± 0.064	>252	3.37
21		0.175 ± 0.041	80.50 (67.65 - 113.9)	460	0.226 ± 0.053	356	3.51
22		0.295 ± 0.083	64.77 (53.46 - 80.16)	220	0.347 ± 0.041	187	3.51
23		0.263 ± 0.029	65.20 (52.13 - 87.97)	248	0.305 ± 0.009	214	3.51
24		0.116 ± 0.035	64.16 (54.50 - 76.87)	553	0.155 ± 0.017	417	3.76
25		0.152 ± 0.041	>100	>658	0.218 ± 0.056	>458	3.31

26		0.172 ± 0.080	>100	>581	0.227 ± 0.034	>441	2.87
27		0.468 ± 0.036	>100	>213	0.575 ± 0.030	>173	2.42
28		0.130 ± 0.030	>100	>769	0.218 ± 0.062	>459	2.89
29		0.190 ± 0.029	>100	>526	0.301 ± 0.036	>332	2.97

^aData represent mean ± standard deviation of three independent experiments. Chloroquine (CQ) was used as positive control (IC₅₀ D10 = 0.020 ± 0.004 μM; W2 = 0.271 ± 0.082 μM). The CC₅₀ and associated 95% confidence interval from the merged data sets from at least three independent experiments for THP-1 cells. Selectivity index (SI): IC₅₀ toward the parasite compared with compound cytotoxicity IC₅₀ on host cells (CC₅₀/IC₅₀). ^bMarvin/JChem 20.9 was used to calculate logD (distribution coefficient) or logP (partition coefficient) values, ChemAxon (<https://www.chemaxon.com>).

Assessment of *In-Vitro* Early ADME-Tox Profile

The entire compound library was investigated for potential early toxicity-related issues exploiting a high throughput screening platform in order to assess the compound safety. Compounds **1-30** were tested in a panel of *in-vitro* assays including CYP3A4, to investigate drug-drug interactions, and hERG, to evaluate potential cardiotoxicity associated with the inhibition of the potassium channel, which plays a key role in cardiac rhythm regulation. Early evaluation of hERG toxicity has been strongly recommended by both the United States Food and Drug Administration (FDA) and the European Medicines Agency (EMA) to avoid hERG interactions and identify safe molecules.⁴⁰ Among the different cytochrome P450 isoenzymes, CYP3A4 was selected as it is considered the most promiscuous human CYP enzyme, contributing to the metabolism of more than 50% of all marketed drugs and being frequently involved in unwanted drug-drug interactions.⁴¹ In addition, our ADME-Tox panel included cytotoxicity assays using human A549 and HEK293 cell lines, to preliminary evaluate toxicity. The compounds were screened in each assay to determine their % Effect at 10 μM. A traffic light system⁴²⁻⁴⁴ (Figure 3) was used to rank compounds with % Effect in presence of a tested compound: green denotes <50 % Effect, yellow denotes 51-89 % Effect, and red denotes >90 % Effect. This system allowed for easy visualization and rapid decision making for SAR study and compound selection. Almost all compounds presented a safe CYP3A4 profile (<50% Inhibition at 10 μM), with the broad-spectrum

antiparasitic agents **24** and **27** showing an improved safety profile with respect to their parental compound **19** (Inhibition CYP3A4 **19** = 49%; **24** = 25%; **27** = 22%, Table S1 and Figure 3). Only the 4*H*-1,2,4-triazole (**2**) and thiazole (**5**) derivatives displayed a % of CYP3A4 inhibition > 50% (58 and 53%, respectively). The entire library presented an overall negligible hERG inhibition and an ideal profile (green), with the exception of compound **24** which showed an acceptable profile (yellow: 50% inhibition, Figure 3 and Table S1). Interestingly, none of the compounds turned out to be cytotoxic in A549 and HEK293 cell lines.

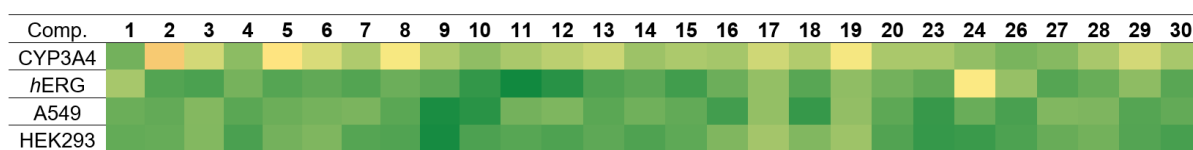
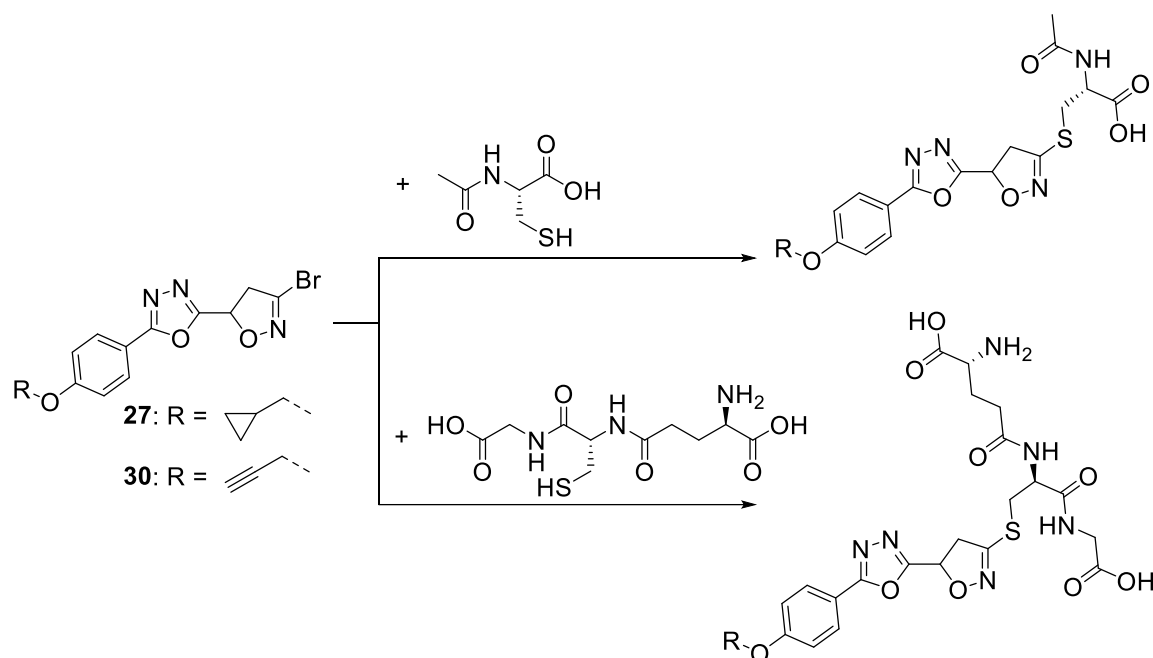


Figure 3. Early *in-vitro* ADME-tox properties of the compound library. All the assays were performed at 10 μ M compound concentration. The data are reported as a traffic light system. An ideal compound would be expected to be associated with a green colour. Green: preferred criteria, % Inhibition: <50 %. Yellow: acceptable criteria, 51-89 % Inhibition. Red: undesirable criteria, >90 % Inhibition. All assay plates passed quality control assessment with Z' value for each assay plate being a minimum value of 0.6. All experiments were performed in independent duplicate or triplicate, and the standard error for each result (% Inhibition) is <10 %. Raw values are reported in **Table S1** of the Supporting Information.

Establishing Reactivity Status of Compounds **27** and **30** with Cellular Thiols

Our compound library presents a 3-bromo-4,5-dihydroisoxazole (BDHI) moiety, which has been proven to be a moderately electrophilic warhead able to covalently react with activated cysteines such as those present in catalytic dyads or triads.⁴⁵⁻⁴⁷ To exclude indiscriminate thiol reactivity, the reactivity of two selected compounds with *N*-acetyl cysteine (NAC) and glutathione (GSH) were assessed. In detail, we selected compound **27**, the most potent anti-*T. brucei* agent, and compound **30**, the chemical probe designed and synthesized for future target(s) identification studies. The compounds (100 μ M) were incubated with an excess of GSH (10 mM) and/or NAC (200 μ M) in ACN/phosphate-buffered saline (PBS, pH 7.4) mixtures, according to their respective solubilities. NAC was chosen as a model

for a non-activated cysteine ($pK_a = 9.52$).⁴⁸ Compared to GSH ($pK_a = 8.83$), NAC has the advantage of not significantly altering the physicochemical properties of **27** and **30** upon adduct formation (see Scheme 3 for chemical structures).



Scheme 3. Reaction of compounds **27** and **30** with NAC and GSH. Chemical structures of parental compounds and formed adducts.

The **27/30**-NAC adducts resulted to be less lipophilic than the parental compounds, and were retained in the RP column allowing adduct detection and analysis. The intrinsic reactivity of compounds **27** and **30** with NAC was assessed using a stoichiometric ratio of 1:2 (in favor of NAC), while a stoichiometric ratio of 1:100 (in favor of GSH) was exploited for the experiments in presence of GSH to mimic a more physiological setting. In the first experimental setting, monitoring of the starting compound was performed, as well as NAC and the adduct formation, while in the presence of GSH, only the starting compound was followed over time. Reaction kinetics and adduct formation (Scheme 3) were monitored by LC-MS as reported in the Experimental section. The $[M+H]^+$ values of the monitored species at the predetermined time points based on the kinetic study design are listed in Table S2 of Supporting Information.

At physiological pH, negligible traces of adducts were formed with both compound **27** and **30** in presence of NAC. The content of the starting compounds remained almost constant over time (Figure 4A-F), up to 24 hr of incubation in all tested conditions. Thus, the BDHI-containing compounds are expected to selectively engage activated cysteines within the active site of biological targets, while avoiding side reactions with cellular thiols.

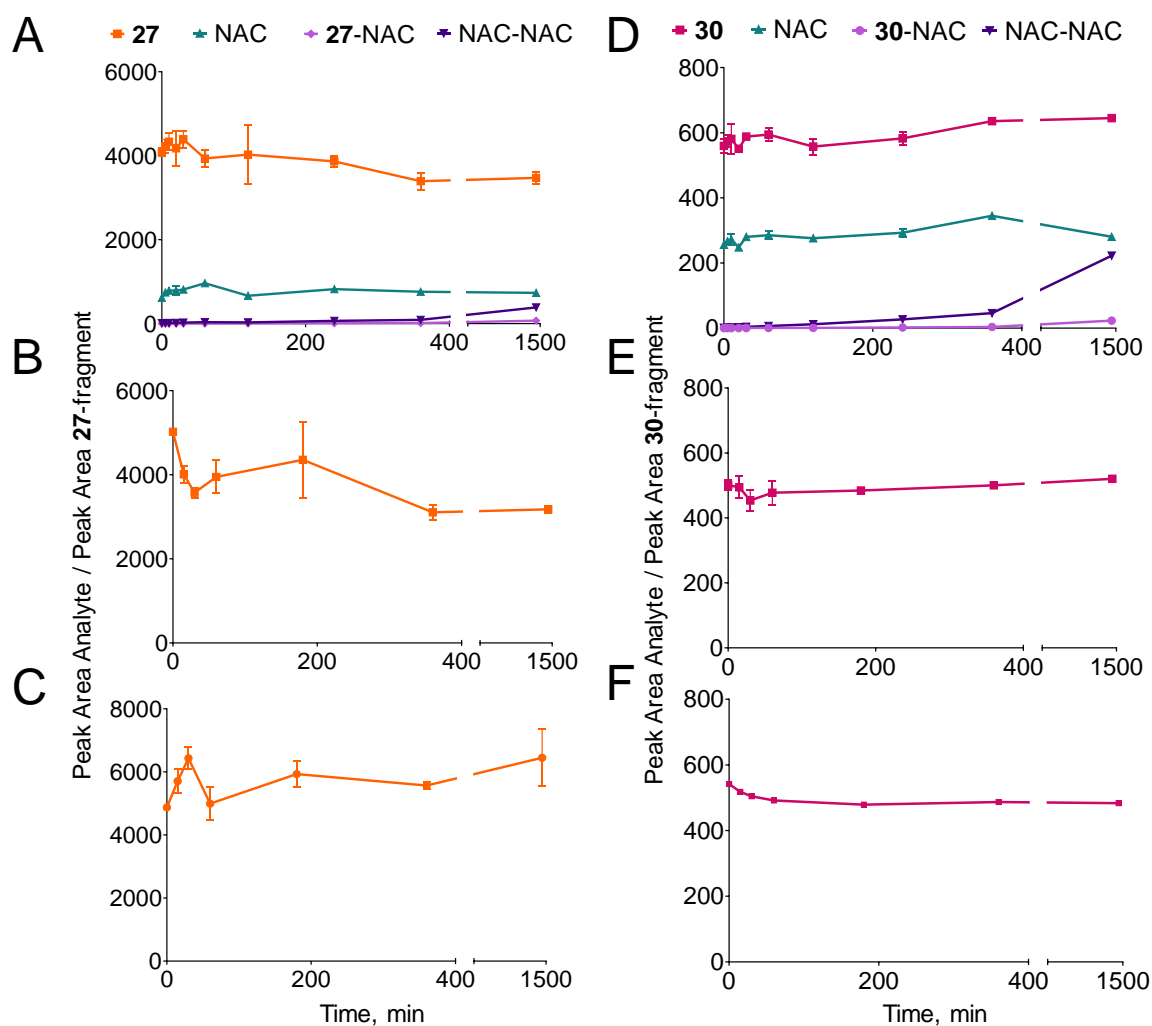


Figure 4. A-F) Kinetic studies of compounds **27** and **30**. **A)** Time-dependent peak areas of (i) compound **27** (orange), (ii) NAC (green), (iii) **27-NAC** adduct (light purple), and (iv) NAC-NAC dimer (dark purple), measured at different times points following the incubation of compound **27** with NAC at a 1:2 stoichiometric ratio. **B, C)** Time-dependent peak areas of compound **27**, measured at different times points following incubation with GSH at a 1:100 stoichiometric ratio (**B**), and measured at different times points following incubation in ACN/phosphate buffer (50:50 % v/v, **C**). **D)** Time-dependent peak areas of (i) compound **30** (pink), (ii) NAC (green), (iii) **30-NAC** adduct (light purple), and (iv) NAC-NAC dimer (dark purple), measured at different times points following the incubation of compound **30** with NAC at a 1:2 stoichiometric ratio. **E, F)** Time-dependent peak areas of (i)

compound **30** (pink), measured at different times points following incubation with GSH at a 1:100 stoichiometric ratio (E), and measured at different times points following incubation in ACN/phosphate buffer (50:50 % v/v, F).

CONCLUSION

Overall, in this work we demonstrated that the 1,3,4-oxadiazole is a privileged scaffold for the development of pan-active antiparasitic agents. Starting from a phenotypic screening of an in-house library, followed by a SAR study around the lipophilic tail of the identified hit (**19**), we discovered the cyclopropyl derivative **27**, as a potent and selective anti-*T. brucei* agent ($IC_{50} = 2.73 \mu M$; $SI > 37$). Compound **27** exhibited a CNS MPO > 5 , fulfilling the requirements for potential BBB penetration and for fighting stage 2 HAT infection. The alkyne-derivative chemical probe **30** maintained the desired antitrypanosomal activity and will be exploited for proteomics experiments aimed at target(s) identification. Due to the presence of the moderately reactive BDHI warhead, enzymes with an activated cysteine in their active sites are expected to be found as targets. In addition, compound **27** displayed a nanomolar potency towards both the CQ-sensitive (D10) and CQ-resistant (W2) *P. falciparum* strains (IC_{50} D10 = $0.468 \mu M$; $SI > 213$; W2 = $0.575 \mu M$, $SI > 173$), and a moderate antileishmanial activity. In parallel, we identified the cyclohexyl-derivative **24** showing low micromolar IC_{50} s towards *T. brucei*, *L. infantum* and *L. tropica* promastigotes (IC_{50} *T. brucei* = $2.41 \mu M$; *L. infantum* = $5.95 \mu M$; and *L. tropica*: $8.98 \mu M$), *L. infantum* amastigotes ($IC_{50} = 8.18 \mu M$), and a nanomolar potency towards both *P. falciparum* strains (IC_{50} D10 = $0.116 \mu M$; $SI = 553$; W2 = $0.155 \mu M$, $SI = 417$). Investigation of early ADME-Tox properties allowed us to prove the safe profile of our compounds. Overall, we characterized novel 1,3,4-oxadiazole derivatives that could pave the way for the development of broad-spectrum antiparasitic agents, widening the therapeutic options and decreasing the global burden of VBPDs.

METHODS

General Information

Reagents were purchased at the highest commercial quality from Sigma-Aldrich or Fluorochem and used without further purification. DBF was prepared according to literature.⁴⁹ 1H NMR and ^{13}C NMR

spectra were recorded with a Varian Mercury 300 (300 MHz) spectrometer. NMR spectra were obtained in deuterated solvents, such as CDCl₃ or DMSO-*d*₆. The chemical shift (δ values) are reported in ppm and corrected to the signal of the deuterated solvents [7.26 ppm (¹H NMR) and 77.16 ppm (¹³C NMR) for CDCl₃; 2.50 ppm (¹H NMR) and 39.52 ppm (¹³C NMR) for DMSO-*d*₆; and 3.31 ppm (¹H NMR) and 49.00 ppm (¹³C NMR) for methanol-*d*₄]. Peak multiplicities are reported as: s (singlet), d (doublet), dd (doublet of doublets), t (triplet), dt (doublet of triplets), q (quartet), m (multiplet), br (broadened). Chemical shifts (δ) are expressed in ppm and coupling constants (*J*) in Hertz (Hz). Thin layer chromatography (TLC) plates were purchased from Sigma-Aldrich (silica gel 60 F254 aluminum sheets, with fluorescence indicator 254 nm) and UV light (254 nm) was used to visualize the compounds. Flash chromatography was performed using silica gel, pore size 60 Å, 230-400 mesh particle size. High-resolution mass spectrometry (HRMS) analyses were performed using the Ultimate 3000 HPLC (Dionex), set to automatically inject into the LTQ Orbitrap XL mass spectrometer (Thermo Fisher Scientific, USA), equipped with an ESI source (Thermo Scientific Inc., Milano, Italia) and operating in full scan mode. Analyses were carried in positive ion mode. The chromatographic purity of final compounds was determined by high performance liquid chromatography (HPLC) analyses on a Waters 1525 Binary HPLC Pump, equipped with a Waters 2489 UV-vis detector (Waters, Milford, MA), using a Symmetry C18 Column (4.6 × 75 mm, 3.5 μm particle size). Solvent A and B (A = Millipore water with 0.1% TFA, B = ACN with 0.1% TFA), and two different methods were used. Method A: gradient elution (85:15 for 0.2 min, 85:15 → 5:95 over 14 min) of the mobile phase consisting of solvents A and B, at a flow rate of 1 mL/min at room temperature. Method B: gradient elution (40:60 for 0.2 min, 40:60 → 5:95 over 14 min) of the mobile phase consisting of solvents A and B, at a flow rate of 1 mL/min at room temperature. The purity of all final compounds was >95%.

The detailed synthetic procedures for the preparation of intermediates and final compounds is reported in Supporting Information.

Parasite Cultures

T. b. brucei Lister 427 bloodstream forms were grown in a humidified incubator at 37 °C, 5% CO₂ in complete HMI-9 medium 1 supplemented with 10% heat-inactivated Fetal Bovine Serum (FBS) and

100 UI/mL penicillin/streptomycin. Parasites maintenance was done in T25 ventilated flasks by subpassage at a concentration of 1×10^4 /mL every 2 days on T25 ventilated flasks.

Promastigote stage of *L. infantum* strain (MHOM/TN/80/IPT1, kindly provided by Dr. M. Gramiccia and Dr. T. Di Muccio, ISS, Roma) and *L. tropica* (MHOM/SY/2012/ISS3130) were cultured in RPMI 1640 medium (EuroClone) supplemented with 10% heat-inactivated fetal calf serum (EuroClone), 20 mM Hepes, and 2 mM L-glutamine at 24 °C.

P. falciparum cultures were carried out according to Trager and Jensen with slight modifications.⁵⁰ The CQ-susceptible strains D10 and the CQ-resistant strain W2 were maintained at 5% hematocrit (human type A-positive red blood cells) in RPMI 1640 (EuroClone) medium with the addition of 1% AlbuMax (Invitrogen, Milan, Italy), 0.01% hypoxanthine, 20 mM Hepes, and 2 mM glutamine. All the cultures were maintained at 37 °C in a standard gas mixture (1% O₂, 5% CO₂, and 94% N₂).

Cell Cultures

Human leukemia cell line, THP-1 (ATCC® TIB-202™) were cultured in RPMI-1640 medium supplemented with 10% heat-inactivated Fetal Bovine Serum (FBS), 2 mM L-glutamine, 100 UI/mL penicillin/streptomycin, 20 mM HEPES. Cell line was maintained in a humidified incubator at 37°C and 5% CO₂ by subculture every three days in 20 ml of media at a concentration of 1×10^5 /ml in a T75 flask. All cell culture reagents were purchased from Lonza-Bioscience (Morrisville, NC).

In Vitro Evaluation of Anti-*T. brucei* Activity

The efficacy of compounds against *T. brucei* bloodstream forms was evaluated using a modified resazurin-based assay previously described in literature.^{43,51} The compounds efficacy against *T. brucei* bloodstream forms was evaluated using a resazurin-based assay. Parasites were added to 100 µL of serial dilutions of compounds in supplemented complete medium at a cell density of 5×10^3 /mL. As a quality control, a dose response curve for the antitrypanosomal pentamidine was included in all the assays. The final volume of the assay is 200 µL/well. Each condition was carried out in duplicate. Following 72h incubation at the specific conditions for each parasite, 20 µL of a 0.5 mM resazurin solution was added and plates were incubated for a further 4 hr under the same conditions. Fluorescence was measured at

544 nm and 590 nm excitation and emission wavelength, respectively, using a Synergy 2 Multi-Mode Reader (Biotek, Winooski, VT, USA). Results were shown as % of parasite growth inhibition compared to control (untreated parasites) and represent the average of at least three independent experiments. The effect was evaluated by the determination of the IC₅₀ value (concentration required to inhibit growth in 50%) and calculated by non-linear regression curves using GraphPad Prism version 8.1.1 for Windows (GraphPad Software, San Diego CA, USA).

Antileishmanial Activity Assay

To estimate the 50% inhibitory concentration (IC₅₀) towards *L. infantum* strain (MHOM/TN/80/IPT1) and *L. tropica* (MHOM/SY/2012/ISS3130) promastigotes, the MTT (3-[4,5-dimethylthiazol-2-yl]-2,5-diphenyltetrazolium bromide) method was used.^{52, 53} Compounds were dissolved in DMSO and then diluted with medium to achieve the required concentrations. Drugs were placed in 96 wells round-bottom microplates and seven serial dilutions made. Parasites were diluted in complete medium to 5×10^6 parasites/mL and 100 μ L of the suspension was seeded into the plates, incubated at 24 °C for 72 h and then 20 μ L of MTT solution (5 mg/mL) was added into each well for 3 hr. The plates were then centrifuged at $1000 \times g$ for 8 min at r.t., the supernatants discarded and the resulting pellets dissolved in 100 μ L of lysing buffer consisting of 20% (w/v) of a solution of SDS (Sigma), 40% of DMF (Merck) in H₂O. The absorbance was measured spectrophotometrically at a test wavelength of 550 nm and a reference wavelength of 650 nm. The results are expressed as IC₅₀ which is the dose of compound necessary to inhibit parasite growth by 50%; each IC₅₀ value is the mean of separate experiments performed in duplicate.

In Vitro Assay Against Intramacrophage amastigotes

THP-1 cells were plated at 5×10^5 cells/mL in 16 Lab-Tek culture slides (Nunc) in 100 μ L and treated with 0.1 μ M PMA for 72 hr to achieve differentiation into macrophages. Cells were then washed and infected with stationary phase *L. infantum* promastigotes at a macrophage/promastigote ratio of 1/10 for 24 hr. Cell monolayers were then washed to remove non-internalized parasites and incubated in the presence of different concentrations of test compounds for 72 hr. Slides were fixed with methanol and

stained with Giemsa. The percentage of infected macrophages in treated and non-treated cells was determined by light microscopy.⁵⁴

Antimalarial Activity Assay

All compounds were dissolved in DMSO and then diluted with medium to achieve the required concentrations (final DMSO concentration <1%, non-toxic to the parasite). Drugs were placed in 96-well flat-bottomed microplates (Corning-Costar) and serial dilutions made. Asynchronous cultures with parasitaemia of 1–1.5% and 1% final hematocrit were aliquoted into the plates and incubated for 72 hr at 37 °C. Parasite growth was determined spectrophotometrically (OD₆₅₀) by measuring the activity of the parasite lactate dehydrogenase (pLDH), according to a modified version of the method of Makler in control and drug-treated cultures.⁵⁵ The antiplasmodial activity is expressed as 50% inhibitory concentrations (IC₅₀); each IC₅₀ value is the mean ± standard deviation of at least three separate experiments performed in duplicate.

Cytotoxicity in THP-1 cells

The cytotoxicity effect of compounds on THP-1-derived macrophages was assessed by the colorimetric MTT assay (3-(4,5-dimethylthiazol-2-yl)-2,5-diphenyl tetrazolium bromide). Briefly, THP-1 cells were suspended in RPMI complete medium at a density of 1x06 cells/mL and 100 µL/well were seeded in a 96-well plate and were differentiated into macrophages by addition of 40 ng/mL of phorbol-myristate 13-acetate (PMA, Sigma, Saint Louis, MI, USA) for 24 hr followed by replacement with fresh medium for more 24 hr. Subsequently, cells were incubated with 100 µL of compounds ranging from 100 to 12.5 µM after dilution in the RPMI complete medium. Each condition was carried out in quadruplicate. After 72 hr of incubation at 37 °C 5% CO₂, the medium was removed and 200 µL of 0.5 mg/mL MTT solution diluted in RPMI was added. Plates were incubated for an additional 4 hr. Then 160 µL of media was removed and the same volume of 2-propanol was added. Absorbance was read at 570 nm using a Synergy 2 Multi-Mode Reader (Biotek, Winooski, VT, USA). Cytotoxicity was evaluated by the determination of the CC₅₀ value (drug concentration that reduced the percentage of viable cells in 50%) and calculated by non-linear regression analysis using GraphPad Prism version

8.1.1 for Windows (GraphPad Software, San Diego, CA, USA). The results represent the average of at least three independent experiments. For each compound, the Selectivity Index (SI) was calculated as the ratio between cytotoxicity in THP-1 (CC₅₀, 72 hr) and activity against parasites (IC₅₀, 72 hr).

Early *in-vitro* ADME-Tox Assays

Chemicals and assay kits. All chemical reagents, cell culture media, and standard inhibitors were of the highest quality and included A549 and HEK293 cell-lines (DSMZ, German Collection of Microorganisms and Cell Cultures, Braunschweig, Germany), penicillin G (P-11-010, PAA Laboratories GmbH, Austria), E-4031 (BML-KC158-0005, Enzo Life Sciences, Inc., Farmingdale, NY, USA), paclitaxel (T7191, Sigma-Aldrich, MO, USA), cytochrome c (C2037, Sigma-Aldrich, MO, USA) and ketoconazole (K1003, Sigma Aldrich, Burlington, MA, USA). Test and reference compounds (except E-4031 being at 3 mM in water) were dissolved to yield 10 mM stock solutions in 100 % v/v DMSO (Carl Roth GmbH & Co. KG, Karlsruhe, Germany) and stored at -20 °C. Assay kits used in the *in-vitro* ADME-Tox assay panel included CellTiter-Glo® reagent for cytotoxicity (G7572, Promega Corp., Madison, WI, USA); Vivid® CYP3A4 Green for Cytochrome P450 3A4 liability (P2857, ThermoFisher Scientific, Carlsbad, CA, USA); Predictor™ *h*ERG for *h*ERG based cardiotoxicity (PV5365, ThermoFisher Scientific, Carlsbad, CA, USA).

Hardware. Screening of compounds were performed in 384-well microtiter plates. A Cell Explorer HTS platform (PerkinElmer, Waltham, MA, USA) equipped with an Echo 550 Liquid Handler (Labcyte, Sunnyvale, CA, USA) and Multidrop (ThermoFisher Scientific, Carlsbad, CA, USA) liquid handling systems were used for low volume compound and bulk reagent addition respectively. Assay measurements were made using an EnVision Multilabel 2103 Reader (PerkinElmer, Waltham, MA, USA) in luminescence mode (cell viability assays), fluorescence intensity mode (CYP3A4 assays) and fluorescence polarization mode (*h*ERG assay).

Data Analysis. The raw data from compounds of screening at 10 µM were analyzed using Excel (Microsoft, Seattle, WA, USA). Raw data from each assay plate were normalized using the respective controls located in an entire column of each assay plate (0.1 % v/v DMSO yielding 0 % Effect in each assay; assay specific reference inhibitor in 0.1 % v/v DMSO yielding 100 % Effect in each assay). Where

necessary, outlier elimination in the control wells was performed using the 3-sigma method. All assay plates underwent quality control assessment following calculation of the Z' value for each assay plate with a minimum value of 0.6.⁵⁶ The % Effect for each compound at 10 μ M was calculated and reported. All experiments were performed in at least duplicate and the standard error for each result (% Effect) is <10 %.

Cytotoxicity Assay

This assay made use of the CellTiter-Glo® which determines the number of viable cells in culture based on quantitation of the ATP present, an indicator of metabolically active cells. A549 cells and HEK293 cells were grown on surface-modified T175 cell culture flasks in Dulbecco's Modified Eagle Medium with 10 % fetal calf serum (FCS), streptomycin (100 μ g/mL), and 100 U/mL penicillin G. Test compounds and the cytotoxicity reference inhibitor (paclitaxel 10 μ M final concentration in 0.1 % v/v DMSO yielding 100 % Effect) and DMSO (final 0.1 % v/v DMSO yielding 0 % Effect) were added in each well of 384-well plates (20 nL/well; 0.1 % v/v DMSO) using the Echo 550 Liquid Handler. At about 80 % confluency, cells were washed, trypsinized, resuspended, and counted in RPMI-1640 medium before seeding in white 384-well microtiter plates (20 μ L) at 500 cells/well. Following incubation for 24 hr at 37 °C in the presence of 5 % CO₂, 20 μ L/well of CellTiter-Glo® reagent was added to each well and incubated for 10 min in the dark, after which plates read using an EnVision Multilabel 2103 Reader.

Cytochrome P450 3A4 Assay

This assay made use of CYP3A4 BACULOSOMES® Plus reagent containing microsomes prepared from insect cells expressing a human P450 isozyme. The CYP3A4 specific substrate (Vivid® DBOMF Substrate) undergoes metabolism by the CYP3A4 into high fluorescence metabolite (excitation 485 nm; emission 520 nm). Test compounds and CYP3A4 reference inhibitor (ketoconazole 10 μ M final concentration in 0.1 % v/v DMSO yielding 100 % Effect) and DMSO (final 0.1 % v/v DMSO yielding 0 % Effect) were added in each well of 384-well plates (5 nL/well in 0.1 % v/v DMSO) using the Echo 550 Liquid Handler. This was followed by addition of 2.5 μ L/well of Vivid® CYP3A4 Green

BACULOSOMES®/Regeneration System mixture and incubated for 20 min at rt, after which the reaction was initiated by addition of 2.5 μ L/well NADP⁺/Substrate. After a further 10 min incubation at rt, the CYP3A4 reaction was stopped by adding 2.5 μ L Tris-Base 0.5 M solution per well and plates read using an EnVision Multilabel 2103 Reader.

*h*ERG Cardiotoxicity Assay

The Predictor™ *h*ERG fluorescence polarization assay kit makes use of a membrane fraction containing *h*ERG channel protein (Predictor™ *h*ERG Membrane) and a high-affinity red fluorescent *h*ERG channel ligand, or “tracer” (Predictor™ *h*ERG Tracer Red), in a homogenous, fluorescence polarization-based format (excitation 531 nm; emission 1 (S-pol) 579 nm; emission 2 (P-pol) 579 nm; Dichroic Mirror (D555fp/D595)). When Predictor™ *h*ERG Tracer Red is bound by the *h*ERG channel protein, the tracer produces a high fluorescence polarization. Compounds that bind to the *h*ERG channel protein (competitors) are identified by their ability to displace the tracer, resulting in a lower fluorescence polarization. Test compounds (10 nL/well in 0.1 % v/v DMSO), *h*ERG reference inhibitor (E-4031) at 30 μ M (100 nL/well in 0.1 % v/v DMSO yielding 100 % Effect) and DMSO (final 0.1 % v/v DMSO yielding 0 % Effect) were added to 384-well plates using an Echo 550 Liquid Handler system. To each well of an assay plate, 5 μ L Predictor™ *h*ERG Membrane solution (undiluted) and 5 μ L “tracer” (1 nM final concentration in assay) were added. The plates were incubated for 2 hr at 25 °C in a humidified incubator with fluorescence polarization measured using an EnVision Multilabel 2103 Reader.

Kinetic Studies at Physiological pH

Chemicals. Ultrapure water was prepared by a Milli-Q purification system (Millipore, Bedford, MA, USA). *N*-Acetylcysteine (NAC), Glutathione (GSH), sodium dihydrogen phosphate and phosphoric acid, formic acid (FA), acetonitrile (all ultrapure 99.5% grade solvents) used in LC-MS analysis were provided by Sigma-Aldrich (Milan, Italy).

Sample preparation. Compounds **27** and **30** (100 μ M) were incubated at 37°C with gentle shaking (500 RPM, using a benchtop ThermoMixer, Eppendorf) with, respectively, an excess of GSH (10 mM)

and NAC (200 μ M) in ACN/phosphate buffer (PBS, pH 7.4) (50:50 %v/v), according to compound solubility. For both compounds, an aliquot was taken from each reaction mixture at different set time points (0, 5, 10, 20, 30 min and 1, 2, 3, 6 and 24 hr) and diluted in H₂O/FA (100:0.2) to stop the reaction. Further dilution in H₂O/FA (100:0.1) was performed to achieve the initial condition in the chromatographic gradient. Finally, the samples were filtered with a 0.45 μ m PTFE membrane to remove particulate matter, transferred to vials and injected in triplicates into the liquid chromatography-mass spectrometry (LC-MS) system.

LC-HRMS analysis. The analytical platform used comprises the Ultimate 3000 HPLC (Dionex), coupled to an LTQ Orbitrap XL mass spectrometer (Thermo Fisher Scientific, USA). The chromatographic separation was performed using a reverse phase Agilent Zorbax SB-C18 column (150 \times 2.1 mm, i.d. 3.5 μ m, CPS analitica, Milan, Italy) with a 20 minutes linear gradient of mobile phase A (H₂O/FA, 100/0.1, %v/v) and B (ACN/FA, 100/0.1, %v/v) starting from a 5% to a final 95% of B phase with a 200 μ L/min flow. For the GSH samples, a 5-minute divert valve exclusion was added to the LC method to avoid the injection of high amounts of unreacted GSH to the MS system. An LTQ Orbitrap XL mass spectrometer equipped with an ESI source was used as analyzer, working in FullMS (MS1) mode only. The spectra were acquired in positive ion mode. Xcalibur 4.0 was used for instrument control and spectra analysis.

Data analysis. Using Xcalibur 4.0, the extracted ion chromatograms for the $[M+H]^+$ values of the monitored species were used to obtain the corresponding Area Under the Curve (AUC). The chosen peak algorithm was Genesis, and Gaussian smoothing was enabled with 9 points. An ordinary one-way ANOVA test was performed in GraphPad comparing the ratio (Peak Area BDHI-containing compound / Peak Area BDHI-containing compounds-fragment) calculated at each set time points against time 0 values, operating the Multi-comparison analysis.

ASSOCIATED CONTENT

Supporting Information

Supporting information is available at <http://pubs.acs.org>

Early ADME-Tox data of compounds **1-30** (Table S1); $[M+H]^+$ values of the monitored species in kinetic experiments (Table S2); Detailed synthetic procedures for the preparation of intermediates and final compounds; ^1H NMR Spectra; ^{13}C NMR Spectra; HRMS Spectra; HPLC Chromatograms; Final Compounds (Chemical Structures); Intermediates (Chemical Structures); References.

AUTHOR INFORMATION

Corresponding Author

Chiara Borsari, Phone: +39 02503 19309.

E-mail: chiara.borsari@unimi.it

Notes: conflicts of interest

The manuscript was written through contributions of all authors. All authors have given approval to the final version of the manuscript.

ACKNOWLEDGEMENTS

This publication is based upon work from COST Action CA21111 “One Health drugs against parasitic vector borne diseases in Europe and beyond (OneHealthdrugs)”, supported by COST (European Cooperation in Science and Technology). We are grateful to the Immunohematology and Transfusion Medicine Service, Department of Laboratory Medicine, and ASST Grande Ospedale Metropolitano Niguarda (Milan) for providing the erythrocytes for parasite cultures.

Funding Sources

C.B. is grateful for the support by L'Oréal-UNESCO for Women in Science. N.S. is an assistant researcher funded by national funds through FCT and co-funded through the European Social Fund within the Human Potential Operating Programme 2021.04285.CEECIND. P.C., N.B., S.P., A.A. are grateful to the UNIMI GSA-IDEA project for financial support.

ABBREVIATIONS USED

HAT, Human African Trypanosomiasis; *T. brucei*, *Trypanosoma brucei*; *L. infantum*, *Leishmania infantum*; *P. falciparum*, *Plasmodium falciparum*; BBB, blood brain barrier; CNS, central nervous system; DCM, dichloromethane; ACN, acetonitrile; THF, tetrahydrofuran; EtOH, Ethanol; DIPEA, *N,N*-diisopropylethylamine; NAC, *N*-acetylcysteine; GSH, glutathione; WHO, World Health Organization; VBPDs, vector-borne parasitic diseases; PBS, phosphate-buffered saline; CC₅₀, half-maximal cytotoxicity concentration; THP-1, human monocytic cell line; A549, human lung adenocarcinoma epithelial cell line; HEK293, human embryonic kidney 293 cells; hERG, human Ether-à-go-go-Related Gene.

REFERENCES

1. Shirley, H.; Grifferty, G.; Yates, E. F.; Raykar, N.; Wamai, R.; McClain, C. D. The Connection between Climate Change, Surgical Care and Neglected Tropical Diseases. *Ann Glob Health* **2022**, *88* (1), 68. doi: 10.5334/aogh.3766
2. Büscher, P.; Cecchi, G.; Jamonneau, V.; Priotto, G. Human African trypanosomiasis. *Lancet* **2017**, *390* (10110), 2397-2409. doi: 10.1016/s0140-6736(17)31510-6
3. Landi, G.; Linciano, P.; Borsari, C.; Bertolacini, C. P.; Moraes, C. B.; Cordeiro-da-Silva, A.; Gul, S.; Witt, G.; Kuzikov, M.; Costi, M. P.; Pozzi, C.; Mangani, S. Structural Insights into the Development of Cycloguanil Derivatives as Trypanosoma brucei Pteridine-Reductase-1 Inhibitors. *ACS Infect Dis* **2019**, *5* (7), 1105-1114. doi: 10.1021/acsinfecdis.8b00358
4. Barrett, M. P.; Burchmore, R. J.; Stich, A.; Lazzari, J. O.; Frasc, A. C.; Cazzulo, J. J.; Krishna, S. The trypanosomiasis. *Lancet* **2003**, *362* (9394), 1469-1480. doi: 10.1016/s0140-6736(03)14694-6
5. Pisarski, K. The Global Burden of Disease of Zoonotic Parasitic Diseases: Top 5 Contenders for Priority Consideration. *Trop Med Infect Dis* **2019**, *4* (1), 44. doi: 10.3390/tropicalmed4010044
6. Zekar, L.; Sharman, T. Plasmodium falciparum Malaria. In *StatPearls*, StatPearls Publishing. Copyright © 2024, StatPearls Publishing LLC.
7. Nagle, A. S.; Khare, S.; Kumar, A. B.; Supek, F.; Buchynskyy, A.; Mathison, C. J.; Chennamaneni, N. K.; Pendem, N.; Buckner, F. S.; Gelb, M. H.; Molteni, V. Recent developments in drug discovery for leishmaniasis and human African trypanosomiasis. *Chem Rev* **2014**, *114* (22), 11305-11347. doi: 10.1021/cr500365f
8. Borsari, C.; Quotadamo, A.; Ferrari, S.; Venturelli, A.; Cordeiro-da-Silva, A.; Santarem, N.; Costi, M. P., Chapter Two - Scaffolds and Biological Targets Avenue to Fight Against Drug Resistance in Leishmaniasis. In *Annual Reports in Medicinal Chemistry*, Botta, M., Ed. Academic Press: 2018, 51, 39-95.
9. Ma, Z.; Augustijn, K.; De Esch, I.; Bossink, B. Public-private partnerships influencing the initiation and duration of clinical trials for neglected tropical diseases. *PLoS Negl Trop Dis* **2023**, *17* (11), e0011760. doi: 10.1371/journal.pntd.0011760
10. Moraes, C. B.; Witt, G.; Kuzikov, M.; Ellinger, B.; Calogeropoulou, T.; Prousis, K. C.; Mangani, S.; Di Pisa, F.; Landi, G.; Iacono, L. D.; Pozzi, C.; Freitas-Junior, L. H.; Dos Santos Pascoalino, B.; Bertolacini, C. P.; Behrens, B.; Keminer, O.; Leu, J.; Wolf, M.; Reinshagen, J.; Cordeiro-da-Silva, A.; Santarem, N.; Venturelli, A.; Wrigley, S.; Karunakaran, D.; Kebede, B.; Pöhner, I.; Müller, W.; Panecka-Hofman, J.; Wade, R. C.; Fenske, M.; Clos, J.; Alunda, J. M.; Corral, M. J.; Uliassi, E.; Bolognesi, M. L.; Linciano, P.; Quotadamo, A.; Ferrari, S.; Santucci, M.; Borsari, C.; Costi, M. P.; Gul, S. Accelerating Drug Discovery Efforts for Trypanosomatid Infections Using an Integrated Transnational Academic Drug Discovery Platform. *SLAS Discov* **2019**, *24* (3), 346-361. doi: 10.1177/2472555218823171
11. Bernhard, S.; Kaiser, M.; Burri, C.; Mäser, P. Fexinidazole for Human African Trypanosomiasis, the Fruit of a Successful Public-Private Partnership. *Diseases* **2022**, *10* (4), 90. doi: 10.3390/diseases10040090
12. Rahi, M.; Sharma, A. India could harness public-private partnerships to achieve malaria elimination. *Lancet Reg Health Southeast Asia* **2022**, *5*, 100059. doi: 10.1016/j.lansea.2022.100059
13. Gilbert, I. H. Drug discovery for neglected diseases: molecular target-based and phenotypic approaches. *J Med Chem* **2013**, *56* (20), 7719-7726. doi: 10.1021/jm400362b
14. Borsari, C.; Jiménez-Antón, M. D.; Eick, J.; Bifeld, E.; Torrado, J. J.; Olías-Molero, A. I.; Corral, M. J.; Santarem, N.; Baptista, C.; Severi, L.; Gul, S.; Wolf, M.; Kuzikov, M.; Ellinger, B.; Reinshagen, J.; Witt, G.; Linciano, P.; Tait, A.; Costantino, L.; Luciani, R.; Tejera Nevado, P.; Zander-Dinse, D.; Franco, C. H.; Ferrari, S.; Moraes, C. B.; Cordeiro-da-Silva, A.;

- Ponterini, G.; Clos, J.; Alunda, J. M.; Costi, M. P. Discovery of a benzothiophene-flavonol halting miltefosine and antimonial drug resistance in Leishmania parasites through the application of medicinal chemistry, screening and genomics. *Eur J Med Chem* **2019**, *183*, 111676. doi: 10.1016/j.ejmech.2019.111676
15. Borsari, C.; Santarem, N.; Macedo, S.; Jiménez-Antón, M. D.; Torrado, J. J.; Olías-Molero, A. I.; Corral, M. J.; Tait, A.; Ferrari, S.; Costantino, L.; Luciani, R.; Ponterini, G.; Gul, S.; Kuzikov, M.; Ellinger, B.; Behrens, B.; Reinshagen, J.; Alunda, J. M.; Cordeiro-da-Silva, A.; Costi, M. P. SAR Studies and Biological Characterization of a Chromen-4-one Derivative as an Anti-Trypanosoma brucei Agent. *ACS Med Chem Lett* **2019**, *10* (4), 528-533. doi: 10.1021/acmedchemlett.8b00565
 16. Uliassi, E.; Piazzini, L.; Belluti, F.; Mazzanti, A.; Kaiser, M.; Brun, R.; Moraes, C. B.; Freitas-Junior, L. H.; Gul, S.; Kuzikov, M.; Ellinger, B.; Borsari, C.; Costi, M. P.; Bolognesi, M. L. Development of a Focused Library of Triazole-Linked Privileged-Structure-Based Conjugates Leading to the Discovery of Novel Phenotypic Hits against Protozoan Parasitic Infections. *ChemMedChem* **2018**, *13* (7), 678-683. doi: 10.1002/cmdc.201700786
 17. Magoulas, G. E.; Afroudakis, P.; Georgikopoulou, K.; Roussaki, M.; Borsari, C.; Fotopoulou, T.; Santarem, N.; Barrias, E.; Tejera Nevado, P.; Hachenberg, J.; Bifeld, E.; Ellinger, B.; Kuzikov, M.; Fragiadaki, I.; Scoulica, E.; Clos, J.; Gul, S.; Costi, M. P.; de Souza, W.; Prousis, K. C.; Cordeiro da Silva, A.; Calogeropoulou, T. Design, Synthesis and Antiparasitic Evaluation of Click Phospholipids. *Molecules* **2021**, *26* (14), 4204. doi: 10.3390/molecules26144204
 18. Neau, P.; Hänel, H.; Lameyre, V.; Strub-Wourgaft, N.; Kuykens, L. Innovative Partnerships for the Elimination of Human African Trypanosomiasis and the Development of Fexinidazole. *Trop Med Infect Dis* **2020**, *5* (1), 17. doi: 10.3390/tropicalmed5010017
 19. Lindner, A. K.; Lejon, V.; Chappuis, F.; Seixas, J.; Kazumba, L.; Barrett, M. P.; Mwamba, E.; Erphas, O.; Akl, E. A.; Villanueva, G.; Bergman, H.; Simarro, P.; Kadima Ebeja, A.; Priotto, G.; Franco, J. R. New WHO guidelines for treatment of gambiense human African trypanosomiasis including fexinidazole: substantial changes for clinical practice. *Lancet Infect Dis* **2020**, *20* (2), e38-e46. doi: 10.1016/s1473-3099(19)30612-7
 20. Jacobs, R. T.; Nare, B.; Wring, S. A.; Orr, M. D.; Chen, D.; Sligar, J. M.; Jenks, M. X.; Noe, R. A.; Bowling, T. S.; Mercer, L. T.; Rewerts, C.; Gaukel, E.; Owens, J.; Parham, R.; Randolph, R.; Beaudet, B.; Bacchi, C. J.; Yarleth, N.; Plattner, J. J.; Freund, Y.; Ding, C.; Akama, T.; Zhang, Y. K.; Brun, R.; Kaiser, M.; Scandale, I.; Don, R. SCYX-7158, an orally-active benzoxaborole for the treatment of stage 2 human African trypanosomiasis. *PLoS Negl Trop Dis* **2011**, *5* (6), e1151. doi: 10.1371/journal.pntd.0001151
 21. Betu Kumeso, V. K.; Kalonji, W. M.; Rembry, S.; Valverde Mordt, O.; Ngolo Tete, D.; Prêtre, A.; Delhomme, S.; Ilunga Wa Kyhi, M.; Camara, M.; Catusse, J.; Schneitter, S.; Nusbaumer, M.; Mwamba Miaka, E.; Mahenzi Mbembo, H.; Makaya Mayawula, J.; Layba Camara, M.; Akwaso Massa, F.; Kaninda Badibabi, L.; Kasongo Bonama, A.; Kavunga Lukula, P.; Mutanda Kalonji, S.; Mariero Philemon, P.; Mokilifi Nganyonyi, R.; Embana Mankiara, H.; Asuka Akongo Nguba, A.; Kobo Muanza, V.; Mulenge Nasandhel, E.; Fifi Nzeza Bambuwu, A.; Scherrer, B.; Strub-Wourgaft, N.; Tarral, A. Efficacy and safety of acoziborole in patients with human African trypanosomiasis caused by Trypanosoma brucei gambiense: a multicentre, open-label, single-arm, phase 2/3 trial. *Lancet Infect Dis* **2023**, *23* (4), 463-470. doi: 10.1016/s1473-3099(22)00660-0
 22. Peña, I.; Pilar Manzano, M.; Cantizani, J.; Kessler, A.; Alonso-Padilla, J.; Bardera, A. I.; Alvarez, E.; Colmenarejo, G.; Cutillo, I.; Roquero, I.; de Dios-Anton, F.; Barroso, V.; Rodriguez, A.; Gray, D. W.; Navarro, M.; Kumar, V.; Sherstnev, A.; Drewry, D. H.; Brown, J. R.; Fiandor, J. M.; Julio Martin, J. New compound sets identified from high throughput phenotypic screening against three kinetoplastid parasites: an open resource. *Sci Rep* **2015**, *5*, 8771. doi: 10.1038/srep08771

23. Thomas, M. G.; De Rycker, M.; Ajakane, M.; Albrecht, S.; Álvarez-Pedraglio, A. I.; Boesche, M.; Brand, S.; Campbell, L.; Cantizani-Perez, J.; Cleghorn, L. A. T.; Copley, R. C. B.; Crouch, S. D.; Daugan, A.; Drewes, G.; Ferrer, S.; Ghidelli-Disse, S.; Gonzalez, S.; Gresham, S. L.; Hill, A. P.; Hindley, S. J.; Lowe, R. M.; MacKenzie, C. J.; MacLean, L.; Manthri, S.; Martin, F.; Miguel-Siles, J.; Nguyen, V. L.; Norval, S.; Osuna-Cabello, M.; Woodland, A.; Patterson, S.; Pena, I.; Quesada-Campos, M. T.; Reid, I. H.; Revill, C.; Riley, J.; Ruiz-Gomez, J. R.; Shishikura, Y.; Simeons, F. R. C.; Smith, A.; Smith, V. C.; Spinks, D.; Stojanovski, L.; Thomas, J.; Thompson, S.; Underwood, T.; Gray, D. W.; Fiandor, J. M.; Gilbert, I. H.; Wyatt, P. G.; Read, K. D.; Miles, T. J. Identification of GSK3186899/DDD853651 as a Preclinical Development Candidate for the Treatment of Visceral Leishmaniasis. *J Med Chem* **2019**, *62* (3), 1180-1202. doi: 10.1021/acs.jmedchem.8b01218
24. Thompson, A. M.; O'Connor, P. D.; Blaser, A.; Yardley, V.; Maes, L.; Gupta, S.; Launay, D.; Martin, D.; Franzblau, S. G.; Wan, B.; Wang, Y.; Ma, Z.; Denny, W. A. Repositioning Antitubercular 6-Nitro-2,3-dihydroimidazo[2,1-b][1,3]oxazoles for Neglected Tropical Diseases: Structure-Activity Studies on a Preclinical Candidate for Visceral Leishmaniasis. *J Med Chem* **2016**, *59* (6), 2530-2550. doi: 10.1021/acs.jmedchem.5b01699
25. Wijnant, G. J.; Croft, S. L.; de la Flor, R.; Alavijeh, M.; Yardley, V.; Brailard, S.; Mowbray, C.; Van Bocxlaer, K. Pharmacokinetics and Pharmacodynamics of the Nitroimidazole DNDI-0690 in Mouse Models of Cutaneous Leishmaniasis. *Antimicrob Agents Chemother* **2019**, *63* (9), e00829-19. doi: 10.1128/aac.00829-19
26. Schmitt, E. K.; Ndayisaba, G.; Yeka, A.; Asante, K. P.; Grobusch, M. P.; Karita, E.; Mugerwa, H.; Asiimwe, S.; Oduro, A.; Fofana, B.; Doumbia, S.; Su, G.; Csermak Renner, K.; Venishetty, V. K.; Sayyed, S.; Straimer, J.; Demin, I.; Barsainya, S.; Boulton, C.; Gandhi, P. Efficacy of Cipargamin (KAE609) in a Randomized, Phase II Dose-Escalation Study in Adults in Sub-Saharan Africa With Uncomplicated Plasmodium falciparum Malaria. *Clin Infect Dis* **2022**, *74* (10), 1831-1839. doi: 10.1093/cid/ciab716
27. Yeung, B. K.; Zou, B.; Rottmann, M.; Lakshminarayana, S. B.; Ang, S. H.; Leong, S. Y.; Tan, J.; Wong, J.; Keller-Maerki, S.; Fischli, C.; Goh, A.; Schmitt, E. K.; Krastel, P.; Francotte, E.; Kuhen, K.; Plouffe, D.; Henson, K.; Wagner, T.; Winzeler, E. A.; Petersen, F.; Brun, R.; Dartois, V.; Diagana, T. T.; Keller, T. H. Spirotrihydro beta-carbolines (spiroindolones): a new class of potent and orally efficacious compounds for the treatment of malaria. *J Med Chem* **2010**, *53* (14), 5155-5564. doi: 10.1021/jm100410f
28. Rottmann, M.; McNamara, C.; Yeung, B. K.; Lee, M. C.; Zou, B.; Russell, B.; Seitz, P.; Plouffe, D. M.; Dharia, N. V.; Tan, J.; Cohen, S. B.; Spencer, K. R.; González-Páez, G. E.; Lakshminarayana, S. B.; Goh, A.; Suwanarusk, R.; Jegla, T.; Schmitt, E. K.; Beck, H. P.; Brun, R.; Nosten, F.; Renia, L.; Dartois, V.; Keller, T. H.; Fidock, D. A.; Winzeler, E. A.; Diagana, T. T. Spiroindolones, a potent compound class for the treatment of malaria. *Science* **2010**, *329* (5996), 1175-1180. doi: 10.1126/science.1193225
29. LaMonte, G. M.; Rocamora, F.; Marapana, D. S.; Gnädig, N. F.; Otilie, S.; Luth, M. R.; Worgall, T. S.; Goldgof, G. M.; Mohunlal, R.; Santha Kumar, T. R.; Thompson, J. K.; Vigil, E.; Yang, J.; Hutson, D.; Johnson, T.; Huang, J.; Williams, R. M.; Zou, B. Y.; Cheung, A. L.; Kumar, P.; Egan, T. J.; Lee, M. C. S.; Siegel, D.; Cowman, A. F.; Fidock, D. A.; Winzeler, E. A. Pan-active imidazolopiperazine antimalarials target the Plasmodium falciparum intracellular secretory pathway. *Nat Commun* **2020**, *11* (1), 1780. doi: 10.1038/s41467-020-15440-4
30. Galbiati, A.; Zana, A.; Coser, C.; Tamborini, L.; Basilico, N.; Parapini, S.; Taramelli, D.; Conti, P. Development of Potent 3-Br-isoxazoline-Based Antimalarial and Antileishmanial Compounds. *ACS Med Chem Lett* **2021**, *12* (11), 1726-1732. doi: 10.1021/acsmchemlett.1c00354
31. Wager, T. T.; Hou, X.; Verhoest, P. R.; Villalobos, A. Moving beyond rules: the development of a central nervous system multiparameter optimization (CNS MPO) approach to enable alignment of druglike properties. *ACS Chem Neurosci* **2010**, *1* (6), 435-449. doi: 10.1021/cn100008c

32. Wager, T. T.; Hou, X.; Verhoest, P. R.; Villalobos, A. Central Nervous System Multiparameter Optimization Desirability: Application in Drug Discovery. *ACS Chem Neurosci* **2016**, *7* (6), 767-775. doi: 10.1021/acschemneuro.6b00029
33. Boström, J.; Hogner, A.; Llinàs, A.; Wellner, E.; Plowright, A. T. Oxadiazoles in medicinal chemistry. *J Med Chem* **2012**, *55* (5), 1817-1830. doi: 10.1021/jm2013248
34. Milinkevich, K. A.; Yoo, C. L.; Sparks, T. C.; Lorsbach, B. A.; Kurth, M. J. Synthesis and biological activity of 2-(4,5-dihydroisoxazol-5-yl)-1,3,4-oxadiazoles. *Bioorg Med Chem Lett* **2009**, *19* (19), 5796-5798. doi: 10.1016/j.bmcl.2009.07.139
35. Mengeş, N.; Balci, M. Catalyst-Free Hydrogenation of Alkenes and Alkynes with Hydrazine in the Presence of Oxygen. *Synlett* **2014**, *25*, 671-676.
36. Borsari, C.; Corfu, A. I.; Conti, P. Understanding Intrinsic Warhead Reactivity and Cysteine Druggability in Covalent Drug Discovery: Medicinal Chemistry and Chemical Biology Highlights. *CHIMIA* **2023**, *77* (5), 349-352. doi: 10.2533/chimia.2023.349
37. Byun, D. P.; Ritchie, J.; Jung, Y.; Holewinski, R.; Kim, H. R.; Tagirasa, R.; Ivanic, J.; Weekley, C. M.; Parker, M. W.; Andresson, T.; Yoo, E. Covalent Inhibition by a Natural Product-Inspired Latent Electrophile. *J Am Chem Soc* **2023**, *145* (20), 11097-11109. doi: 10.1021/jacs.3c00598
38. Galbiati, A.; Zana, A.; Borsari, C.; Persico, M.; Bova, S.; Tkachuk, O.; Corfu, A. I.; Tamborini, L.; Basilico, N.; Fattorusso, C.; Bruno, S.; Parapini, S.; Conti, P. Role of Stereochemistry on the Biological Activity of Nature-Inspired 3-Br-Acivicin Isomers and Derivatives. *Molecules* **2023**, *28* (7), 3172. doi: 10.3390/molecules28073172
39. Manzano, J. I.; Konstantinović, J.; Scaccabarozzi, D.; Perea, A.; Pavić, A.; Cavicchini, L.; Basilico, N.; Gamarro, F.; Šolaja, B. A. 4-Aminoquinoline-based compounds as antileishmanial agents that inhibit the energy metabolism of Leishmania. *Eur J Med Chem* **2019**, *180*, 28-40. doi: 10.1016/j.ejmech.2019.07.010
40. Garrido, A.; Lepailleur, A.; Mignani, S. M.; Dallemagne, P.; Rochais, C. hERG toxicity assessment: Useful guidelines for drug design. *Eur J Med Chem* **2020**, *195*, 112290. doi: 10.1016/j.ejmech.2020.112290
41. Ekroos, M.; Sjögren, T. Structural basis for ligand promiscuity in cytochrome P450 3A4. *Proc Natl Acad Sci U S A* **2006**, *103* (37), 13682-13687. doi: 10.1073/pnas.0603236103
42. Uliassi, E.; Fiorani, G.; Krauth-Siegel, R. L.; Bergamini, C.; Fato, R.; Bianchini, G.; Carlos Menéndez, J.; Molina, M. T.; López-Montero, E.; Falchi, F.; Cavalli, A.; Gul, S.; Kuzikov, M.; Ellinger, B.; Witt, G.; Moraes, C. B.; Freitas-Junior, L. H.; Borsari, C.; Costi, M. P.; Bolognesi, M. L. Crassiflorone derivatives that inhibit Trypanosoma brucei glyceraldehyde-3-phosphate dehydrogenase (TbGAPDH) and Trypanosoma cruzi trypanothione reductase (TcTR) and display trypanocidal activity. *Eur J Med Chem* **2017**, *141*, 138-148. doi: 10.1016/j.ejmech.2017.10.005
43. Borsari, C.; Luciani, R.; Pozzi, C.; Poehner, I.; Henrich, S.; Trande, M.; Cordeiro-da-Silva, A.; Santarem, N.; Baptista, C.; Tait, A.; Di Pisa, F.; Dello Iacono, L.; Landi, G.; Gul, S.; Wolf, M.; Kuzikov, M.; Ellinger, B.; Reinshagen, J.; Witt, G.; Gribbon, P.; Kohler, M.; Keminer, O.; Behrens, B.; Costantino, L.; Tejera Nevado, P.; Bifeld, E.; Eick, J.; Clos, J.; Torrado, J.; Jiménez-Antón, M. D.; Corral, M. J.; Alunda, J. M.; Pellati, F.; Wade, R. C.; Ferrari, S.; Mangani, S.; Costi, M. P. Profiling of Flavonol Derivatives for the Development of Antitrypanosomatidic Drugs. *J Med Chem* **2016**, *59* (16), 7598-7616. doi: 10.1021/acs.jmedchem.6b00698
44. Linciano, P.; Cullia, G.; Borsari, C.; Santucci, M.; Ferrari, S.; Witt, G.; Gul, S.; Kuzikov, M.; Ellinger, B.; Santarém, N.; Cordeiro da Silva, A.; Conti, P.; Bolognesi, M. L.; Roberti, M.; Prati, F.; Bartocchini, F.; Retini, M.; Piersanti, G.; Cavalli, A.; Goldoni, L.; Bertozzi, S. M.; Bertozzi, F.; Brambilla, E.; Rizzo, V.; Piomelli, D.; Pinto, A.; Bandiera, T.; Costi, M. P. Identification of a 2,4-diaminopyrimidine scaffold targeting Trypanosoma brucei pteridine

- reductase 1 from the LIBRA compound library screening campaign. *Eur J Med Chem* **2020**, *189*, 112047. doi: 10.1016/j.ejmech.2020.112047
45. Byun, D. P.; Ritchie, J.; Jung, Y.; Holewinski, R.; Kim, H. R.; Tagirasa, R.; Ivanic, J.; Weekley, C. M.; Parker, M. W.; Andresson, T.; Yoo, E. Covalent Inhibition by a Natural Product-Inspired Latent Electrophile. *J Am Chem Soc* **2023**, *145* (20), 11097-11109. doi: 10.1021/jacs.3c00598
 46. Galbiati, A.; Bova, S.; Pacchiana, R.; Borsari, C.; Persico, M.; Zana, A.; Bruno, S.; Donadelli, M.; Fattorusso, C.; Conti, P. Discovery of a spirocyclic 3-bromo-4,5-dihydroisoxazole covalent inhibitor of hGAPDH with antiproliferative activity against pancreatic cancer cells. *Eur J Med Chem* **2023**, *254*, 115286. doi: 10.1016/j.ejmech.2023.115286
 47. Bruno, S.; Pinto, A.; Paredi, G.; Tamborini, L.; De Micheli, C.; La Pietra, V.; Marinelli, L.; Novellino, E.; Conti, P.; Mozzarelli, A. Discovery of covalent inhibitors of glyceraldehyde-3-phosphate dehydrogenase, a target for the treatment of malaria. *J Med Chem* **2014**, *57* (17), 7465-7471. doi: 10.1021/jm500747h
 48. Aldini, G.; Altomare, A.; Baron, G.; Vistoli, G.; Carini, M.; Borsani, L.; Sergio, F. N-Acetylcysteine as an antioxidant and disulphide breaking agent: the reasons why. *Free Radic Res* **2018**, *52* (7), 751-762. doi: 10.1080/10715762.2018.1468564
 49. Vyas, D. M.; Chiang, Y.; Doyle, T. W. A short, efficient total synthesis of (\pm) acivicin and (\pm) bromo-acivicin. *Tetrahedron Letters* **1984**, *25* (5), 487-490. doi: [https://doi.org/10.1016/S0040-4039\(00\)99918-0](https://doi.org/10.1016/S0040-4039(00)99918-0)
 50. Trager, W.; Jensen, J. B. Human malaria parasites in continuous culture. *Science* **1976**, *193* (4254), 673-675. doi: 10.1126/science.781840
 51. Di Pisa, F.; Landi, G.; Dello Iacono, L.; Pozzi, C.; Borsari, C.; Ferrari, S.; Santucci, M.; Santarem, N.; Cordeiro-da-Silva, A.; Moraes, C. B.; Alcantara, L. M.; Fontana, V.; Freitas-Junior, L. H.; Gul, S.; Kuzikov, M.; Behrens, B.; Pöhner, I.; Wade, R. C.; Costi, M. P.; Mangani, S. Chroman-4-One Derivatives Targeting Pteridine Reductase 1 and Showing Anti-Parasitic Activity. *Molecules* **2017**, *22* (3), 426. doi: 10.3390/molecules22030426
 52. Mosmann, T. Rapid colorimetric assay for cellular growth and survival: application to proliferation and cytotoxicity assays. *J Immunol Methods* **1983**, *65* (1-2), 55-63. doi: 10.1016/0022-1759(83)90303-4
 53. Baiocco, P.; Ilari, A.; Ceci, P.; Orsini, S.; Gramiccia, M.; Di Muccio, T.; Colotti, G. Inhibitory Effect of Silver Nanoparticles on Trypanothione Reductase Activity and Leishmania infantum Proliferation. *ACS Med Chem Lett* **2011**, *2* (3), 230-233. doi: 10.1021/ml1002629
 54. Konstantinović, J.; Videnović, M.; Orsini, S.; Bogojević, K.; D'Alessandro, S.; Scaccabarozzi, D.; Terzić Jovanović, N.; Gradoni, L.; Basilico, N.; Šolaja, B. A. Novel Aminoquinoline Derivatives Significantly Reduce Parasite Load in Leishmania infantum Infected Mice. *ACS Med Chem Lett* **2018**, *9* (7), 629-634. doi: 10.1021/acsmchemlett.8b00053
 55. Makler, M. T.; Hinrichs, D. J. Measurement of the lactate dehydrogenase activity of Plasmodium falciparum as an assessment of parasitemia. *Am J Trop Med Hyg* **1993**, *48* (2), 205-210. doi: 10.4269/ajtmh.1993.48.205
 56. Zhang, J. H.; Chung, T. D.; Oldenburg, K. R. A Simple Statistical Parameter for Use in Evaluation and Validation of High Throughput Screening Assays. *J Biomol Screen* **1999**, *4* (2), 67-73. doi: 10.1177/108705719900400206

Insert Table of Contents artwork here

